UNITED NATIONS UNIVERSITY
GEOTHERMAL TRAINING PROGRAMME
Orkustofnun, Grensasvegur 9,
IS-108 Reykjavik, Iceland

Reports 2013
Number 24

BOREHOLE GEOLOGY AND HYDROTHERMAL ALTERATION MINERALOGY OF WELL OW-39A, OLKARIA GEOTHERMAL PROJECT, NAIVASHA, KENYA

Joyce Atieno Okoo
Kenya Electricity Generating Company, Ltd.
Olkaria Geothermal Project
P.O. Box 785-20117, Naivasha,
KENYA
jokoo@kengen.co.ke

ABSTRACT

Well OW-39A is a directional well drilled to the south at an azimuth of 180° and inclination of 20° to a measured depth (MD) of 3066 m, adjacent to the Ololbuttot N-S trending eruptive fissure. Comprehensive binocular and petrographic analyses of cuttings from the well indicate that the lithology of the well comprises five rock units, i.e. pyroclasts, rhyolites, tuffs, basalts, and trachytes and then intrusions of rhyolitic, syenitic, basaltic, and granitic composition. Trachyte forms the main reservoir rock and it is the dominant rock below 900 m. These rock units host secondary hydrothermal mineral assemblages which are dependent on temperature, permeability and rock type. Mineral deposition sequences in the well show systematic evolution from low to high temperature conditions with depth, as observed from alteration minerals in veins and vesicles. Five alteration zones were identified: an unaltered zone (0-134 m), a zeolite- smectite-illite zone (134-578 m), a chlorite-illite zone (578-748 m), an epidote-chlorite-illite zone (748-896 m) and an actinolite-epidote-wollastonite zone (896-3066). The appearance of epidote at 750 m and actinolite at 896 m indicates temperatures of 250 and 280°C, respectively, at these depths. A comparison of fluid inclusion analyses, alteration and formation temperature indicates two geothermal episodes, one of a high temperature geothermal system below 700-800 m depth and a recent second phase of cooling. Permeability is observed in the cuttings by the intensity of oxidation, veining, alteration intensity, circulation losses, the presence of calcite, and an abundance of pyrite. Eight feed zones are identified in the well starting from 750 down to 2750 m, deduced from the shape of temperature profiles, and their locations correlate with the cutting data as mentioned above. The intermediate feed zone at 1100 and the major feed zone at the 2100 m are considered the dominant ones in the well.

1. INTRODUCTION

1.1 General information

The Greater Olkaria Geothermal Area (GOGA) is situated southwest of Lake Naivasha in the eastern arm of the African Rift Valley in Kenya (Figure 1). The rift is part of the East African Rift system that

runs from the Afar triple junction at the Gulf of Aden in the north to Beira, Mozambique in the south (Lagat 2004).

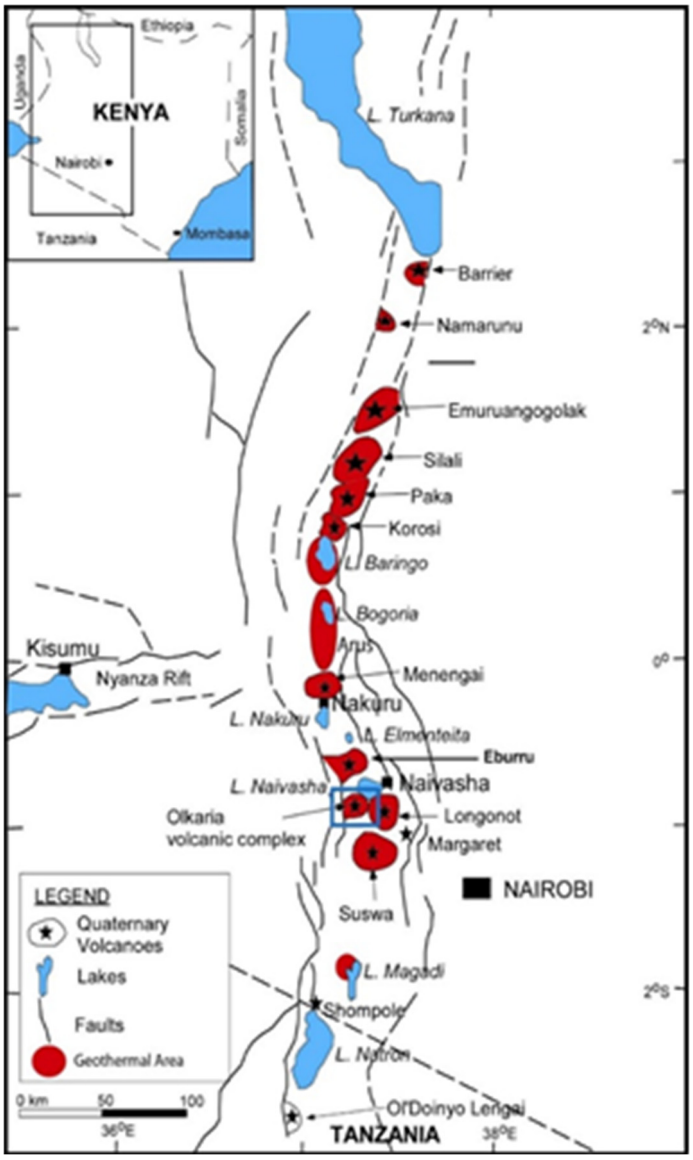

FIGURE 1: Map of Kenya showing the location of Olkaria geothermal field and other Quaternary volcanoes along the rift axis

This segment of the eastern arm of the rift, also called the Kenyan Rift, extends from Lake Turkana in Northern Kenya, where the earliest volcanic rocks in the Kenyan Rift have been found (MacDonald et al., 2001), to Lake Natron in northern Tanzania. The Rift is part of a divergent zone where spreading occurs, resulting in thinning of the crust, eruption of lavas and associated volcanic activities. It crosses two regions of topographic uplift, the Ethiopian and Kenyan Domes, both regarded as the surface manifestation of underlying mantle plumes (Thiessen et al., 1979). The Kenya Dome is associated with more than 1 km of uplift, but is apparently in isostatic equilibrium, supported by the loading of an anomalous mantle within the underlying lithosphere (Smith, 1994). The Olkaria volcanic complex is bounded to the north by the Eburru complex and to the east and south by the Longonot and Suswa volcanoes, respectively. Olkaria geothermal field is divided into smaller sectors (Figure 2) namely: East, Northeast, West, South, Domes and Central Olkaria, all relative to the position of the Olkaria volcanic centre and for ease of development. Power production started in Olkaria East field in 1981 where the first 15 MWe power plant was commissioned. Currently, the production is 45 MWe. Olkaria II power plant, located in the Olkaria Northeast field, was opened in 2003 and currently produces 105 MWe. The third plant, located in Olkaria Northwest field, owned by OrPower, an independent power producer, generates 48 MWe. Currently, construction is underway for Olkaria I (140 MWe) units 4 and 5 in Olkaria East field and Olkaria IV (140 MWe) units 1 and 2 in Domes field (Figure 2).

1.2 Well OW-39A

Well OW-39A is located in the Olkaria East production field, (Figure 2) defined by UTM E 0198168, N 9901777 and an elevation of 2158 m a.s.l. It is a directional well drilled to the south at an azimuth of N 180°E and an inclination of 20° to a measured depth (MD) of 3066 m. The surface, anchor and production casings were set at 50.2, 292, and 750 m, respectively. It was designed as a production well with the aim of tapping steam from Ololbutot fissure, which is a N-S trending eruptive fissure, and also to confirm the importance of this structure, given the fact that it is associated with the most active surface manifestations in Olkaria.

2. GEOLOGY

2.1 Geological setting

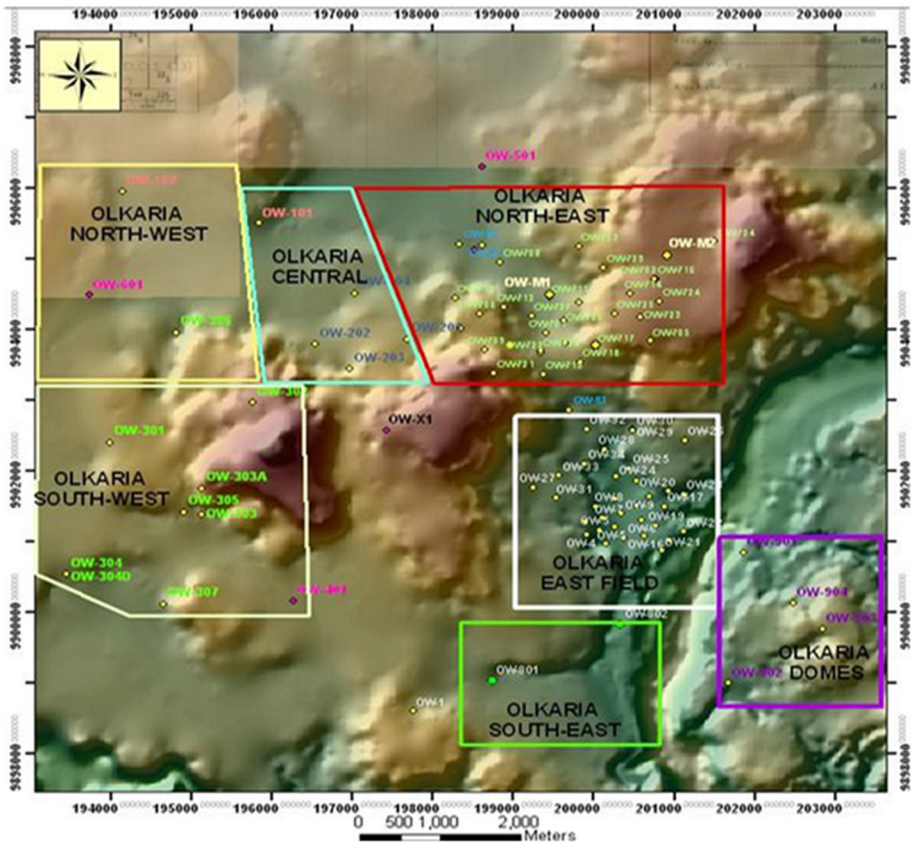

Figure 2: Location map of Well OW-39A and geothermal fields in the Greater Olkaria geothermal area (KenGen, 2000)

According to Baker et al. (1971, 1972) and Smith and Mosley (1993), the African Rift is structurally controlled and was formed due to tectonic activities involving faulting and fracturing at the collisional zones between the Archean Tanzania craton and the Proterozoic orogenic belts. The Greater Olkaria volcanic complex, which is located in the African Rift, is characterized by numerous volcanic centres of Quaternary age (Macdonald et al., 1987; Marshall et al. 2009). These volcanic centres appear as steep-sided domes formed by successions of lavas and/or pyroclastic rocks, or as thick lava flows of restricted lateral extent. Magmatic activities, associated with this complex, commenced during the late Pleistocene and continue to Recent times, as indicated by the Ololbutot comendite lava, which has been dated at 180±50 yrs B.P (Clarke et al., 1990). It is the only occurrence of surface comendite within the Kenya Rift (Lagat, 2004).

Other Quaternary volcanic centres adjacent to the Olkaria Volcanic complex include Longonot volcano to the east, Suswa caldera to the south, and the Eburru volcanic complex to the north (Figure 1). Whereas the other volcanoes are associated with calderas of varying sizes, the Olkaria volcanic complex does not have a clear caldera subsidence structure. The presence of a ring of volcanic domes in the east, south, and southwest (Figure 3) has been used to invoke the presence of a buried caldera (Naylor, 1972; Virkir, 1980; Clarke et al., 1990; Mungania, 1992). Seismic wave attenuation studies for the whole of the Olkaria area have also indicated an anomaly in an area coinciding with the proposed caldera (Simiyu et al., 1998). Other studies on Olkaria have not identified the existence of the caldera, e.g. resistivity studies did not map a clear discontinuity at the margin of the proposed caldera (Onacha, 1993). Ignimbrite flows that could have been associated with the caldera collapse have not been positively identified in Olkaria (Omenda, 1998). Furthermore, petrochemistry of lavas within the Olkaria area shows that they were produced from discrete magma chambers (Omenda, 2000). Another explanation for the proposed caldera hypothesis is that the ring structure was formed by magmatic stresses in the Olkaria "magma chamber" with the line of weakness being loci for volcanism (Omenda, 2000).

2.2 Structural geology

The geological structures (Figure 3) within the Greater Olkaria volcanic complex include: the ring structure, rift fault systems, the Ol'Njorowa gorge, and dyke swarms. The faults trend ENE-WSW, N-

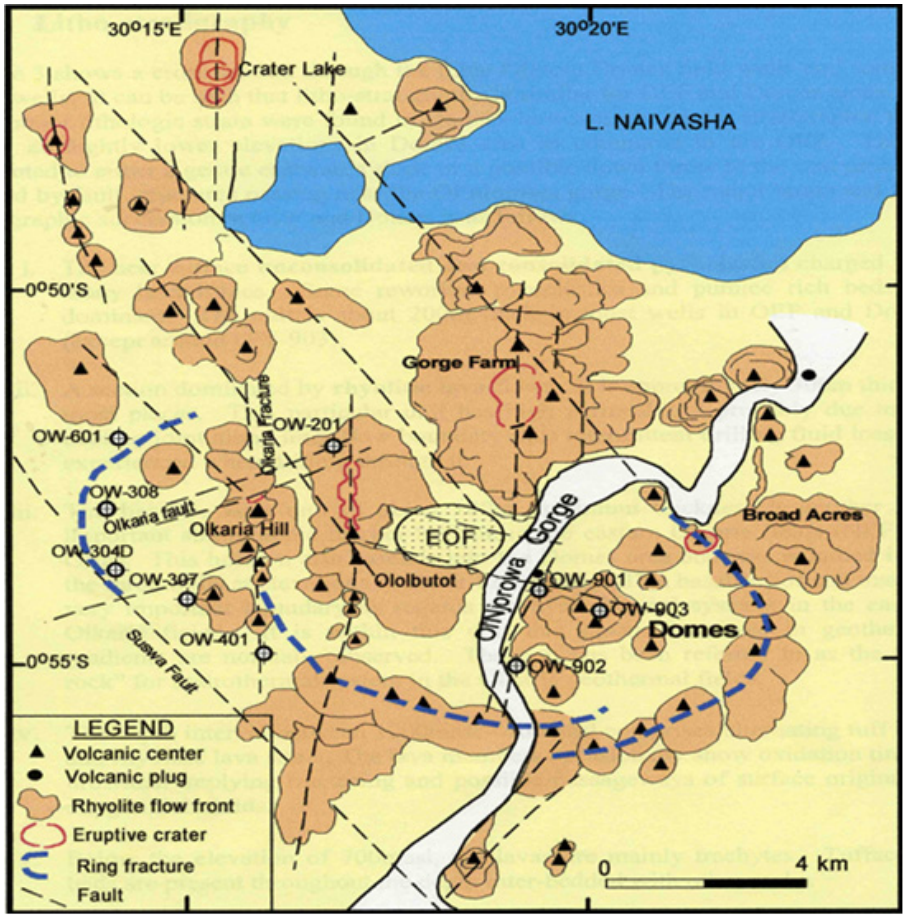

FIGURE 3: Structural map of Greater Olkaria geothermal area (modified from KenGen, 2000)

S, NNE-SSW, NW-SE and WNW-ESE. These faults are more prominent in the East, Northeast and West Olkaria fields, but are scarce in the Olkaria Domes area, possibly due to the thick pyroclastic cover (Lagat, 2004). The NW-SE and WNW-ESE faults are thought to be the oldest fault system and they link the parallel rift basins to the main extensional zone (Wheeler and Karson, 1994). Gorge Farm fault is the most prominent of these faults. It bounds the geothermal fields in the northeast part and extends to the Olkaria Domes area. The most recent structures are the N-S (Ololbuttot eruptive fissure) and the NNE-SSW faults. Dyke swarms exposed in the Ol'Njorowa gorge trend in a north-northeasterly direction, further attesting to the recent reactivation of faults with that trend. The development of the Ol'Njorowa gorge was initiated by faulting along the trend of the gorge but the feature, as it is seen today, was mainly formed due to a catastrophic outflow of Lake Naivasha during its high stands (Clarke et al., 1990). Volcanic plugs (necks) and felsic dykes occurring along the gorge further attest to the fault control in the development of this feature. Subsurface faults have been encountered in most Olkaria wells, as reported in geological well reports (Ryder, 1986; Lagat, 1998, 2004; Muchemi, 2000; Otieno and Kubai, 2013; Mwania et al., 2013). Hydroclastic craters located on the northern edge of the Olkaria Domes area mark magmatic explosions which occurred in submerged country (Mungania, 1999). These craters form a row along which the extrapolated caldera rim trace passes.

2.3 Subsurface and surface geology

The subsurface geology of the Olkaria geothermal field can be divided into five broad lithostratigraphic groups (Figure 4) based on age, tectono-stratigraphy and lithology, as revealed by data from more than eighty deep wells in the geothermal area (Omenda, 2000). The formations are: the Proterozoic "basement" formations; Mau tuffs; Plateau Trachytes; Olkaria Basalt; and Upper Olkaria Volcanics.

The basement consists mainly of Proterozoic amphibolite grade gneiss, schists and associated marble and quartzites of the Mozambiquan group (Shackleton, 1986; Mosley, 1993; Smith and Mosley, 1993). The rocks are not exposed in Olkaria. Reflection seismic, gravity and geological correlations indicate that the depth to the "basement" is about 5-6 km in the Central Kenya Rift (Simiyu, 1996; Simiyu and

Keller, 1997). Seismic and gravity studies indicate the presence of a high-density magmatic intrusion in the metamorphic ''basement'' rocks (Baker and Wohlenberg, 1971; Baker et al., 1971; Simiyu, 1996). The Pre-Mau formation is composed of trachytes, basalts and ignimbrites and is not exposed in the area, but there are outcrops on the rift scarps in parts of the southern Kenya Rift. These rocks are directly overlain by the Mau tuffs that are Pliocene in age.

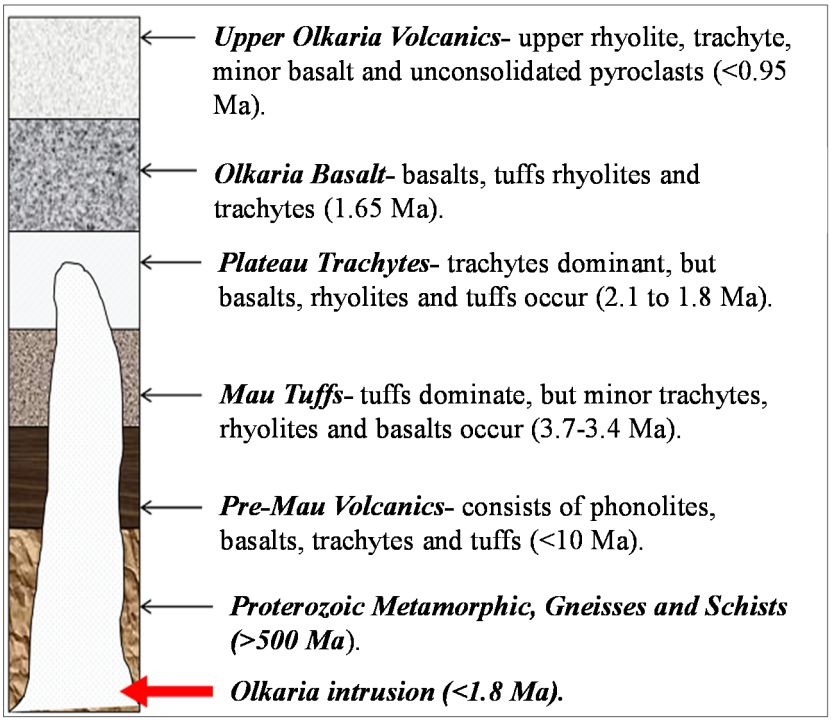

FIGURE 4: Stratigraphic column of the Olkaria volcanic complex (modified from Omenda, 2000)

Mau tuffs are the oldest rocks that are exposed in the Olkaria area. These rocks are common in the area west of Olkaria Hill (Figure 3), but are absent in the east due to an east dipping high angle normal fault that passes through Olkaria Hill (Omenda 1994, 1998). The rocks vary in texture from consolidated to ignimbritic tuffs and are the main geothermal reservoir rocks in the Olkaria west field (Lagat, 2004). Plateau trachytes have been encountered in Olkaria wells and consist mainly of trachytic lavas with intercalations of basalt, tuff and rhyolite. These are of Pleistocene age and occur in the area east of Olkaria Hill where a graben existed prior to their eruptions (Omenda, 1994, 1998). These rocks act as host rock for the Olkaria geothermal field (Ogoso-Odongo, 1986; Omenda, 1994, 1998; Lagat, 2004).

Olkaria basalt is also of Pleistocene age and the formation consists of basaltic flows, separated by thin tuff layers, minor pyroclastic deposits, trachytes and occasional rhyolites. It varies in thickness from 100 m to 500 m, underlying the Upper Olkaria volcanics. From reservoir modelling (Haukwa, 1984; Ambusso and Ouma, 1991) and hydrothermal studies (Browne, 1984; Leach and Muchemi, 1987; Muchemi, 1992; Omenda, 1998) the formation is believed to form the cap-rock of the Olkaria geothermal system.

Upper Olkaria volcanics, which are of mid Pleistocene to Recent age, occur from the surface down to about 500 m depth. They consist of comendite lavas and their pyroclastic equivalents, ashes from Suswa and Longonot volcanoes and minor trachytes and basalts (Thompson and Dodson, 1963; Clarke et al., 1990; Omenda, 1998). Comendite is the dominant rock in this formation. The youngest of these lavas is the Ololbutot comendite, which has been dated at 180±50 yrs (Clarke et al., 1990).

Surface geology of the Olkaria area is dominated by the occurrence of pumice lapilli and ash deposits, which overlie the comendite lava flows. The pyroclastics are well stratified layers and vary from weakly to highly weathered, often imparting a brownish colour to the deposits. The Olkaria volcanic complex has been observed to be the only area within the Kenyan Rift where comenditic lavas occur on the surface (MacDonald et al., 2008; Marshall et al., 2009; Lagat, 2004). These comenditic lavas are exposed in a few locations within Olkaria, notably along lava flow fronts and along Ol'Njorowa gorge.

3. SAMPLING AND ANALYTICAL METHODS

3.1 Sampling

Samples of cuttings from Well OW-39A were taken at each 2 m interval at the drill site during drilling, but in cases where the sample was too small, up to a 4 m depth interval was sampled. Preliminary analysis was done at the rig site by the use of a binocular microscope, to enable the geologists and drillers to understand the subsurface geological formations and conditions, which assisted in applying the right drilling procedures. Representative samples of the rock units encountered in the well were then selected for detailed laboratory analysis of hydrothermal alteration minerals and fluid inclusion studies.

3.2 Analytical methods

3.2.1 Stereo microscope analysis

Drill cuttings sampled at 2 m intervals were scooped from the sample bags using a petri dish. The sample was then washed thoroughly with clean water to remove impurities and dust. Water added onto the cuttings to enhance visibility of the sample and obscure features such as finely disseminated sulphides, e.g. pyrite. The sample was then placed on the mounting stage of an Olympus SX16 binocular microscope for analysis by noting essential features such as: colour(s) of the cuttings, rock type(s), grain size, rock fabrics, original mineralogy, alteration mineralogy and intensity.

3.2.2 Petrographic microscope analysis

Representative samples from selected lithological units encountered in the well were selected and 72 thin sections were prepared for petrographic studies. The thin sections were then mounted on a Leica petrographic microscope for analysis. Petrographic analysis is used to study the mineralogical evolution, confirm the rock type(s), the alteration minerals, and any additional alteration minerals not observed by the binocular microscope.

3.2.3 X-ray diffraction analysis

Samples were selected from representative lithological units and analysed for clays. The <2 microns fractions were prepared for X-ray diffraction by crushing the rock into a fine powder. The crushed sample was placed in a test tube, distilled water was added to dissolve the constituents, then the test tube was shaken and left in a rack so that the <2 microns phyllosilicates were left in suspension. A few drops were placed on a marked glass slide and left to dry so that the sample could be analysed using the XRD equipment. Ethylene glycol was added to the air dried sample and then the sample was heated to between 500-550°C. The samples were analysed in the XRD equipment after each treatment to identify the different types of clays based on the peak locations and the intensity in the XRD spectra.

3.2.4 Fluid inclusion analysis

Fluid inclusions are "bubbles" of fluid trapped within the host mineral during its deposition from its parent hydrothermal fluid. Fluid inclusions can be either primary or secondary. Primary fluid inclusions are trapped in the crystal lattice during growth while secondary fluid inclusions are trapped along healed cracks (Roedder, 1984). Fluid inclusions were identified in the prepared sample by use of a petrographic microscope. Double-polished thin sections (approximately 70 microns) of cuttings from Well OW-39A, which contained abundant quartz, were prepared for fluid inclusion analysis. The thin sections were mounted on a Linkam THS MG 94 heating stage for analysis. The inclusions were heated slowly until the fluid homogenization temperatures (i.e. the bubble disappears) were obtained. Homogenization temperatures of individual inclusions were measured at least twice and the results were recorded in 5°C intervals.

4. RESULTS

4.1 Lithology

The preliminary geological logs of Well OW-39A were done at the rig site where the samples were analysed using binocular microscope, confirmed later in the laboratory using thin section analysis. The lithological column (Figure 5) of the well is composed of unconsolidated pyroclastics forming a thin layer at the top, overlaying a volcanic sequence consisting of tuffs, trachytes, rhyolites, basalt, and some rhyolitic, basaltic, syenitic and granitic intrusions. A summary of the lithology of Well OW-39A are described below.

Pyroclasts 0-14 m
The pyroclastics are unconsolidated and yellowish to brown, light grey and form the upper 14 m in the well. The rock unit consists of lithic fragments of rhyolite, trachyte and pumice. The rock is dominated by volcanic ash, and crystals of glass, quartz, feldspars, obsidian and pumice.

Rhyolites 14-208 m
A 190 m thick formation characterised by rhyolitic lavas and from 100 m depth rhyolitic tuffs. The rhyolitic lava at 14-44 m is whitish to creamish lava microcrystalline with quartz in a fine grained matrix. The lava is slightly quartz and arfvedsonite porphyritic with quartz intergrowth. This is followed by two rhyolitic tuff layers at least 60 m in thickness. The upper tuff is brown in colour and heterogeneous with a lot of quartz in an ashy matrix. The lower tuff is greyish with quartz phenocrysts in a fine matrix. At 158 m depth is a 40 m thick rhyolitic lava, which is white to creamish in colour and well crystallized. The lava is feldspar and quartz rich with phenocrysts of quartz.

Tuffs 232-368 m
This layer consists of a 136 m thick layer of medium grained rhyolitic tuff formation. From 232 to 250 m it is light grey to whitish homogeneous rock with vesicles partially filled. Between 250 to 268 m it is brownish, while from 268-368 m it is greenish heterogeneous rock with lithic fragments of quartz in a fine grained matrix. The rock shows slight oxidation; there is a minor loss between 368 to 374 m.

Basalts 374-414 m
The top 374 to 394 m is composed of a homogeneous non-porphyritic basaltic tuff that is highly fractured, vesicular and there is increased oxidation, veining and an abundance of pyrite. It overlies a 20 m thick basaltic layer characterised by dark brown colour and is fine grained with plagioclase phenocrysts and a lot of magnetite in the matrix. Abundant pyrite appears as cubes embedded in the matrix. Loss of returns was experienced between 414 and 424 m.

Trachyte 424-696 m
This layer is composed of variable trachytic lava. The top 424 to 550 m is brownish fine grained massive and homogeneous non porphyritic lava. The matrix is composed of pyroxenes and microcline laths. Between 550 to 588 m the lava is slightly porphyritic with sanidine and pyroxene. The lava shows veining and the amount of pyrite decreases with depth. This is underlain by ~90 m thick porphyritic layer with a typical trachytic texture. There was a loss of returns between 696 to 748 m.

Basalt 748-762 m
The rock unit is composed of 14 m thick basaltic lava with a loss of returns between 750-758 m. It is dark grey mafic fine to medium grained porphyritic with plagioclase and pyroxenes in a rich very fine grained plagioclase lath. The rock is highly altered and oxidised. Abundant calcite was seen in the vesicles. A medium aquifer is located in this rock unit at 750 m. There was a major loss of returns between 762 to 802 m.

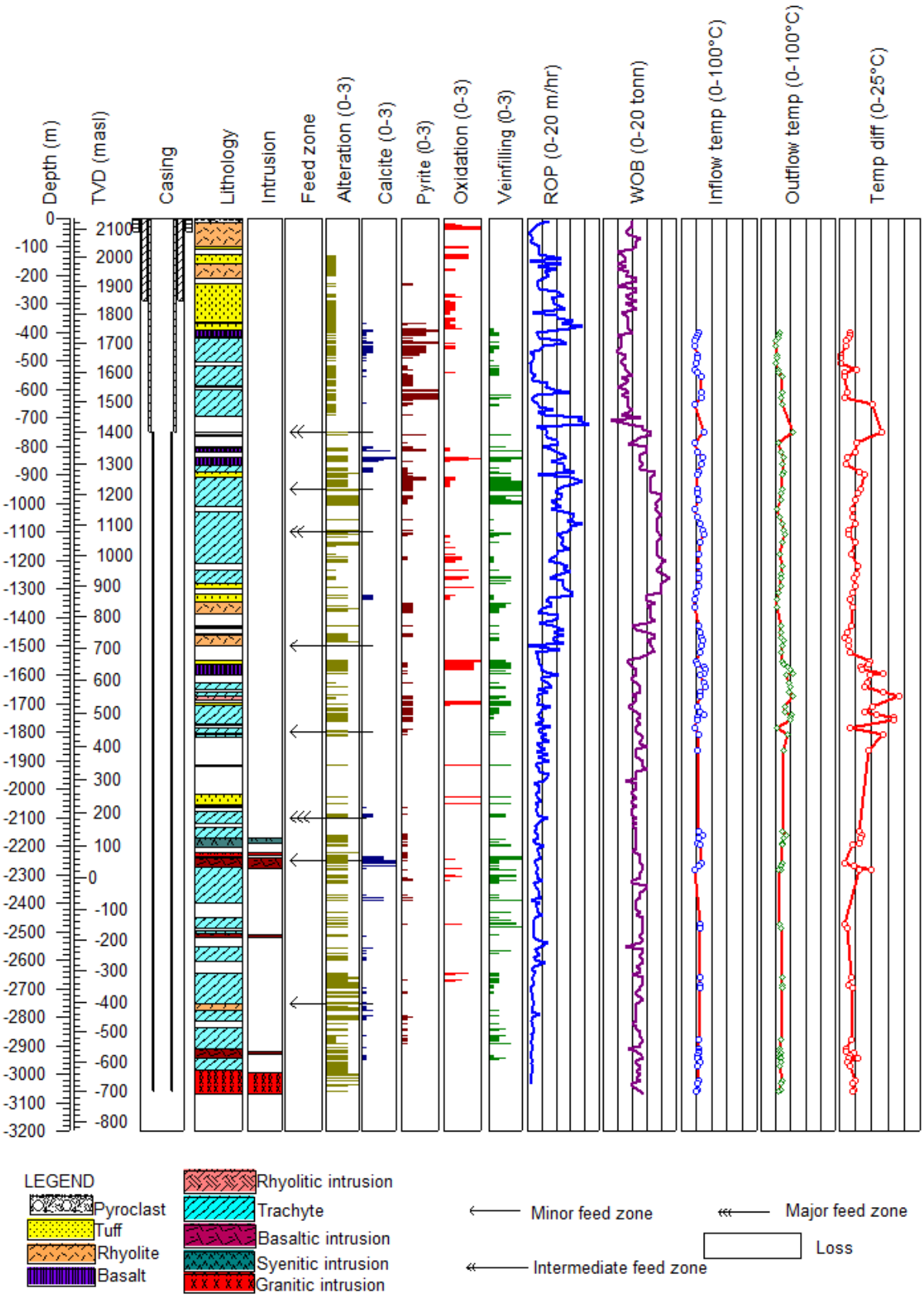

FIGURE 5: Stratigraphy and drilling parameters of Well OW-39A

Trachyte/Basalt 802-1008 m
The top 16 m of this unit is composed of medium grained highly vesicular and homogeneous lava with sanidine phenocrysts. The lava exhibits the flow orientation in the matrix. Pyrite is a common mineral with minor calcite. Veining is common. This unit is underlain by a 40 m thick basaltic layer between 836 and 876 m. The basalt is dark brown, brownish grey fine to medium grained highly oxidised phyric with plagioclase. There is abundant calcite in vesicles and veins. Magnetite is common in the matrix. It is highly altered with an increased abundance of epidote with depth. From 876 to 1008 m the rock is light grey, to light brown medium grained feldspar rich lava sanidine and pyroxene porphyritic, showing increased veining and magnetite with depth. It is intercalating with an 18 m thick heterogeneous highly oxidised and vesicular basaltic tuff between 890 to 908 m.

Trachyte and basaltic tuff 1028-1340 m
This layer consists of trachyte intercalating with less than 50 m thick layers of trachyte. The top depth is a 200 m thick trachyte layer which is a fine to medium grained highly altered grey light grey, light brown feldspar rich lava. It is porphyritic with sanidine and becomes more crystalline with depth. The lava is underlain by a ~50 m dark brown basaltic tuff between 1296 to 1344 m, fine to medium grained with lithic fragments of plagioclase and quartz in the matrix, porphyritic with plagioclase and slightly oxidised. There was a minor loss of returns from 1340 to 1344 m.

Rhyolite 1344-1500 m
This layer is light brown medium grained crystalline less porphyritic with quartz and pyroxenes (augerine). The matrix is composed of quartz; pyrite is disseminated in the matrix and a magnetite vein was noted. The lava is highly altered between 1460 to 1472 m. Between 1500 to 1550 m there was a loss of returns.

Basalt 1550-1602 m
The lava is approximately 40 m thick. The first 12 m is basaltic tuff which is reddish brown heterogeneous with angular grains, highly vesicular and fractured, underlain by a dark brown homogeneous fine to medium grained porphyritic basaltic layer. The rock unit is fractured and veined.

Trachyte 1628-1674 m
Light grey fine to medium grained partially crystalline phyric lava with sanidine and abundant pyroxenes and feldspars in the matrix. It shows flow texture and the feldspar are altered to albite.

Trachyte/basalt 1692-2054 m
Trachyte lava intercalates with thin layers of basalt. Between 1692 to 1710 m is a basaltic layer which is reddish brown, fine grained tuffaceous rock that is highly oxidised. Below this layer lies a trachyte layer which is ~ 200 m thick. The lava is greyish brown, greyish, partially crystalline and porphyritic with quartz, feldspars and pyroxenes. It shows slight oxidation with pyrite disseminated in the matrix. The rock is more altered at 1762-1772 m. The feldspars are altered to albite. At 1916-1920 m and 2020-2054 m is a reddish brown tuffaceous rock with medium heterogeneous angular grains, characterised by high fracturing, veining and oxidation. There is a major loss between 1818-1916 m and 1920-2018 m.

Trachyte 2066-2148 m
Between 2066-2090 m, the lava is light grey, fine grained and less porphyritic. Spherulitic texture is observed and the matrix is composed of feldspars and pyroxene. It is massive and lacks the trachytic texture. The lava is characterised by high fracturing and veining. From 2090 to 2148 m the lava is grey to dark grey, highly porphyritic, shows flow banding and slight oxidation. Abundant epidote was also noted in this layer. Losses occurred at 2120-2134 m.

Trachyte 2240-2750 m
Greyish brown medium grained porphyritic highly altered lava, characterised by a trachytic texture, high veining and fracturing, this layer is 8 m thick (2240-2246 m), overlaying a basaltic intrusion (2248-2274 m described below under intrusives). Beneath the intrusion is a thick layer of trachytic lava (2274-

2750 m) greyish, greyish brown to greyish green, crystalline, highly porphyritic with sanidine and pyroxene (augerine-augite) and shows a flow texture. The matrix is composed of microline laths and pyroxenes and with abundant veins which are completely filled and it is highly altered between 2274 and 2336 m.

Rhyolite 2750-2774 m
Whitish felsic feldspar and quartz rich lava. It is glassy to fine grained with quartz and riebekite phenocrysts. The lava has a high intensity of alteration.

Trachyte 2774-2986 m
This rock unit is fine to medium grained and varies in colour from greyish to brownish. Between 2774 and 2866 m the lava is highly porphyritic with sanidine, quartz and pyroxenes (augerine-augite) and shows typical trachytic texture. From 2866 to 2908 the lava is light grey in colour, more altered and fractured and veined. This lava overlies a ~28 m thick basaltic layer (described below under intrusives). At 2942 -2986 m the lava is greyish brown, medium grained. Veins in this rock unit have been filled. Between 2986 and 3066 m exists a granitic intrusion (discussed below under intrusions).

Intrusions
Intrusions were encountered at depth in the well. They are identified as being relatively fresh compared to the highly altered surrounding host and the chilled margins. The existence of intrusives is indicative of a heat source in a geothermal system. Intrusives encountered in the well are as follows:

Basaltic intrusions
Basaltic intrusives were encountered at 2252-2274, 2504-2518, and 2914-2940 m depth. The intrusives are fine to medium grained, weakly to moderately altered, with glassy margins. They are porphyritic with plagioclase feldspars, and highly fractured. The fresh intrusives are dark grey to black while the altered ones appear grey.

Syenitic intrusion
Syenite occurs at 2170-2190 m. It is light grey to whitish in colour, massive, medium grained and porphyritic with large sanidine phenocrysts. It shows a trachytic texture and the matrix is composed of pyroxenes and feldspars. This intrusion is associated with the major aquifer in the well.

Granitic intrusion
Granite occurs to the bottom of the well from 2992 to 3066 m. It is light grey to whitish, medium to coarse grained with granular and phaneritic texture. The contact with the host rock is glassy and highly altered. The rock is porphyritic with quartz and feldspars and occasionally some individual crystals of quartz form very large phenocrysts. It is massive and fresh with abundant quartz and riebekite in the matrix.

Rhyolitic intrusion
A rhyolitic intrusion was encountered between 1674 and 1686 m. It is a whitish to light grey in colour, medium- to coarse grained, crystalline rock consisting of notable quartz crystals. Arfvedsonite-riebekite and augerine-augite are common in the matrix. The rock is fractured and has veins filled with abundant pyrite.

4.2 Hydrothermal alteration mineralogy

4.2.1 Alteration of primary minerals

Primary minerals are minerals that form during the solidification and crystallization of the rock. These minerals include both the essential minerals used to assign a classification name to a rock and they form in a sequential group as dictated by the physico- chemical conditions under which the magma solidifies.

These minerals become unstable at temperatures prevailing in a geothermal system and, therefore, alter to secondary minerals when subjected to hydrothermal conditions (Browne, 1978). The common primary minerals (Table 1) in this well include volcanic glass, olivine, pyroxene, amphibole, plagioclase, sanidine, microcline and opaques (Fe-Ti oxides).

TABLE 1: Primary minerals; order of replacement and alteration products of Well OW-39A (modified from Browne, 1984)

	Primary minerals	**Alteration product**
Most susceptible	Volcanic glass	Zeolites, clays, chalcedony quartz, calcite
↓	Olivine	Clays, calcite, chlorite, actinolite
	Plagioclase	Calcite, albite, quartz, illite, epidote, sphene
	Sanidine, microcline	Albite, adularia, clays
Least susceptible	Pyroxene	Chlorite, illite, calcite, quartz, albite, epidote
	Opaques	Hematite, pyrite, sphene

4.2.2 Hydrothermal minerals

A number of hydrothermal minerals are highly temperature dependant and are, thus, extensively used to map the temperature regimes of geothermal systems (Browne, 1978, 1984; Omenda, 1998). The hydrothermal alteration minerals appear both as replacements of primary minerals, and as fillings in vesicles, vugs and fractures. The distribution and abundance of the hydrothermal minerals were characterised from binocular microscopic studies, and petrographic and XRD analysis of the drill cutting samples taken at 2 m intervals. Although hydrothermal alteration changed the primary minerals in different ways and magnitude, the original textures and minerals are often still recognizable. The distribution and kind of mineral assemblages present in hydrothermal systems is influenced by factors such as permeability, rock and water composition, temperature, pressure and duration of hydrothermal alteration (Browne and Ellis, 1970; Reyes, 2000). The main hydrothermal minerals encountered in Well OW-39A were oxides (hematite ad magnetite), zeolites (scolecite), quartz, calcite, epidote, pyrite, adularia, wollastonite, fluorite, sphene, albite, actinolite, prehnite and clays (smectite, chlorite, illite, mixed layer clays). The distribution of hydrothermal minerals in Well OW-39A is shown in Figure 6, and a description is given here below:

Hematite was observed as silver-grey, brown to reddish brown in colour. Hematite can form in environments associated with colder in-flow that is more oxygen-rich by the oxidation of magnetite or iron-rich minerals in the formation. In this well, hematite was observed between 274 and 1568 m and is abundant in silver grey below 900 m.

Magnetite is an iron oxide. The reduction of hematite to magnetite at high temperatures and pressures in the presence of water causes the precipitation of stable magnetite from a hydrothermal fluid in a hydrothermal system in vesicles and veins (Mathews, 1976), while magnetite precipitation can also be associated with intrusions. The oxide was first observed at 968 m as a black to brown black cubic mineral filling in veins and occasionally in vesicles.

Zeolites can be distinguished by their shape: mainly fibrous/acicular, tabular/prismatic and granular (Saemundsson and Gunnlaugsson, 2002). The zeolites were observed as white to light brown fibrous and radiating minerals. In this well, zeolites occurred from 134 to 460 m. Zeolites are not common and only scolecite was identified.

Chalcedony is a cryptocrystalline form of silica commonly referred to as the amorphous form of silica. It was observed as translucent white to grey, grey to greyish blue and some were in shades of brown. It was observed in trachyte, basalt and tuffs at the upper parts of the well from 250 m to a depth of about 624 m. Below this depth, it became unstable and recrystallized to quartz. It is a low-temperature

mineral, observed in the well as fillings in veins and vesicles, indicating formation temperatures of ~110 to 180°C.

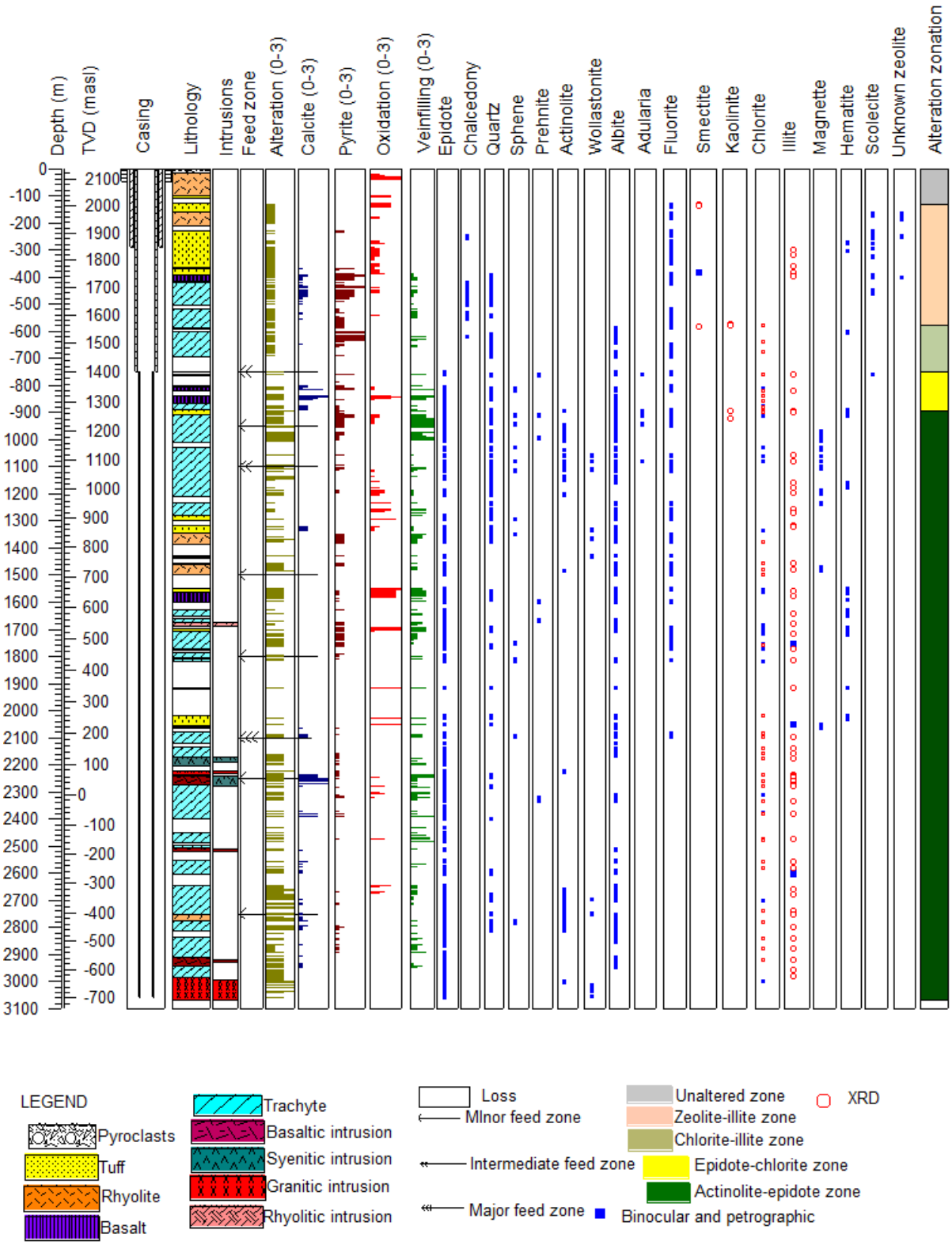

FIGURE 6: Lithology, distribution of hydrothermal minerals and mineral zones in well OW-39A

Quartz first occurred at 400 m as a secondary mineral and was not observed as such below 2812 m. It is colourless and occurs in euhedral to subhedral crystals. It has conchoidal fracturing, indistinct cleavage, and undulating extinction under the microscope which makes it easily identifiable. It occurs as an infilling in both vesicles and veins. The first occurrence of quartz indicates formation temperature greater than 180°C.

Calcite occurs intermittently from 250 m and disappears completely below 2950 m. It is abundant between 836 and 850 m in basaltic rock and 2234 and 2264 m in a fractured trachytic rock at the contact with a basaltic intrusion (2240-2276 m). The major aquifer in this well (2100 m) is associated with calcite in trachytic lava, indicating that the zone is permeable. Calcite replaces feldspars and volcanic glass, and is also seen as an infill in vesicles, fractures and veins. It is abundant in the basaltic formations with minor occurrences in tuffs and trachyte. Browne and Ellis (1970) stated that relatively high carbon dioxide concentrations in solution in the presence of a mineral pH buffer causes calcite to form in place of other calcium alumino-silicates. Therefore, calcite formation in this well could be related to carbon dioxide (CO_2) concentrations in the reservoir fluids. Platy calcite was observed in the vesicles as composite crystals formed of numerous paper thin subcrystals. It was common in the basaltic and trachytic layers between 392 to 750 m and also at 760 m. Its presence in the well indicates possible boiling conditions and high porosity (Browne, 1984; Omenda, 1998; Muchemi, 1992; Simmons and Christenson, 1994). Calcite also disappears at temperatures >300°C (Simmons and Christenson, 1994).

Pyrite occurs as euhedral cubic crystals with shiny brassy yellow lustre. The mineral was first observed at 232 m in the well. Well-formed cubic pyrite crystals were deposited in fractures, vesicles and veins and as disseminations in the groundmass. An abundance of pyrite indicates high activity of sulphur, good permeability and past or present boiling regimes (Lagat, 1998), hence its abundance in the well coincided with intermediate aquifers at 750 and 1100 m, and also a minor aquifer at 950 m, indicating good present and past permeability and also boiling zones at these depths.

Epidote first appeared at 748 m; from there, crystalline epidote persisted to the bottom of the well. The mineral is identified from rock cuttings by its yellow to greenish yellow colours. In thin sections, it is pleochroic with pale green, pale yellow and greenish brown colours exhibiting high relief with parallel extinction. It was found filling fractures, vesicles, and replacing primary plagioclase and pyroxene and, in most cases, formed mineral associations mainly with quartz, chlorite, calcite, actinolite and prehnite and sometimes pyrite. The presence of well-crystallized epidote indicates temperatures of more than 250°C (Omenda, 1990; Gylfadóttir et al., 2011).

Albite forms by the replacement of primary feldspars and plagioclase phenocrysts into hydrothermal albite. It is identified by its colour, which is cloudy white or greyish white. It is an anisotropic mineral showing uneven fracturing. It appears as striated, anhedral to subhedral crystals. It was observed in the well from 588 m down to the bottom; albite replaces feldspars at temperatures of 180°C and above (Reyes, 2000).

Fluorite is a very common mineral in this well. It was first observed at 134 m and was then common down to 2750 m. It is identified in a petrographic microscope by its very low relief, two perfect cleavages and its pale brown to colourless colour in thin section, while it is isotropic under crossed nicols.

Sphene is not a common mineral in this well. It was first encountered at 812 m and appearing intermittently down to 2786 m, where it disappeared completely. It occurs mainly as irregular grains but rarely as clear euhedral crystals having acute rhombic sections. The mineral forms mainly as a result of alteration of Fe-Ti–oxides.

Prehnite was first noted in the well at 758 m. It has a high relief and is colourless in plane polarised light which changes to green yellow and orange in crossed nicols. It is identified by its sheaf like bow-tie texture and strong birefringence. It occurs as vein and vesicle filling in association with epidote and chlorite. Prehnite indicates minimum formation temperatures of about 250°C (Reyes, 2000).

Wollastonite is a rare mineral in this well and appeared first at 1058 m. It is white to colourless, sometimes grey, with a distinct crystal habit appearing as fibrous and radiating aggregates. In thin section it is colourless and has moderately high relief. It forms in vesicles in association with epidote and actinolite. Its presence in the well indicates formation temperatures above 270°C (Reyes, 2000).

Actinolite is pale green, green and sometimes dark green in colour and occurs as fibrous, radial crystals and massive to granular aggregates in the groundmass. In thin sections, it shows moderate relief with weak pleochroism of pale yellow, deep green blue and pale green colours. The first occurrence of actinolite was at 894 m and from there actinolite is persistent to the bottom of the well, filling in vesicles and sometimes seen in veins. The mineral is formed as a replacement of pyroxenes. In most cases it forms mineral associations with quartz, pyrite, wollastonite and epidote. This mineral indicates formation temperatures above 280°C (Lagat, 2007; Gylfadóttir et al., 2011).

Clay minerals

Clay minerals are the most common and dominant hydrothermal alteration minerals that were observed in Well OW-39A. They are finely crystalline or metacolloidal and occur as flake-like or dense aggregates of varying types (Pendon, 2006). Their occurrence in a geothermal system is an indication of changes in the chemical environment, such as the presence of acidic fluids in a relatively neutral environment, while their distribution depends on the ability of fluids to approach equilibrium in host rocks at any scale during the hydrothermal processes (Harvey, 1998) and also as temperature indicators (Kristmannsdóttir, 1979; Franzson, 1998). Four types of clays were identified from the surface to the bottom of the well, based on binocular analysis, petrographic analysis and XRD analysis. A brief description is given below; some XRD analyses are shown in Appendix I.

Smectite is a low temperature clay and it is seen as fine grained brown to green aggregates, recognized by the first order birefringence colour. It was observed at shallow depths, identified by its characteristic extinction sun feature in thin section (384 m). Its occurrence indicates temperatures of less than 200°C (Franzson, 2013) and also an alkaline fluid environment. Smectite is unique in that it swells when ethyl glycol is added to it and, when heated, it shrinks. In this regard, it shows characteristic peaks of 14.78 Å-16.33 Å, 18.37 Å-19.58 Å and 10.50 Å-10.98 Å for air-dried/untreated, glycolated and heated samples, respectively.

Kaolinite is bright green to white in colour, replaces K-feldspar, and occurs as a vein and vesicle filling mineral. It was identified by XRD analysis with a peak of 7.15 Å for the untreated and glycolated samples, and completely collapsed after being heated to 550°C. It occurs in low intensity alteration below 572 m. Kaolinite is associated with acid alteration and low temperatures up to 180°C (Reyes, 2000).

Chlorite is pale green to dark green in cuttings, but in thin sections it is pale green and occasionally shows anomalous brown colour. It is fine to coarse grained weakly to non-pleochroic and shows low birefringence. It exhibits small intergranular patches in the shallow depths while at deeper levels it forms radial aggregates. The mineral occurred as a filling in vesicles, veins and fractures in association with epidote, quartz and calcite. XRD analyses of chlorite showed conspicuous peaks at 7.0-7.2 Å and 14.0-14.5 Å in the untreated, glycolated and oven heated samples, differentiating it from kaolinite whose peak collapses when heated to 550°C.

Illite is a common clay mineral extensively distributed in this well. It is colourless to brown under petrographic microscope. It was observed as a vein filling and as an alteration product of sanidine. Under XRD analyses, it showed strong peaks of between 9.9 and 10.4 Å in untreated, glycol treated and heated samples (Appendix I). It was first observed at 298 m in XRD analysis. Its appearance indicates temperature above 200°C (Kristmannsdóttir, 1979).

4.3 Hydrothermal alteration mineral zonation

Hydrothermal minerals are known to form at specific temperatures in a geothermal system (Browne, 1978, 1984; Omenda, 1998). The distribution of the hydrothermal minerals with depth in Well OW-39A is dependent on temperature. In this well, the mineralization pattern shows five distinct zones, as shown in Table 2. The top zone is the unaltered zone (0-134m) and has no alteration related to geothermal activity, suggesting the temperatures were <40^{o}C. The second zone (zeolite –smectite-illite zone) extends from 134 to 578 m. This is the lowest grade mineral alteration zone, indicating a temperature range of 40-200°C. The upper boundary of this zone coincides with the first occurrence of zeolites at about 134 m. The third zone (Chlorite- illite zone) occurs between 578 to 748 m and is characterised by high oxidation in the upper parts at 600-640 m depth. The upper boundary is marked by the first appearance of chlorite in XRD analysis at 578 m, suggesting the alteration temperatures could be above 230°C. The fourth zone (epidote-chlorite-illite) extends from 748 to 896 m. It is characterised by an abundance of epidote, suggesting that alteration temperatures are above 250°C. Other minerals present in this zone include albite, sphene, quartz, chlorite, illite and calcite. The fifth zone extends from 896 m to the bottom of the well. It is marked by first appearance of actinolite at 896 m, indicating alteration temperatures above 280°C below this depth. It is characterised by mineral assemblages of actinolite, wollastonite, epidote and prehnite. Other minerals in this zone include pyrite, calcite, fluorite, chlorite, illite, and oxides.

TABLE 2: Alteration mineral zones in Well OW-39A

Depth (m)	Alteration	Temp range (^{o}C)
0-134	Unaltered	<40
134-578	Zeolite-smectite-illite	40-200
578 -748	Chlorite-illite	230-250
748-896	Epidote-chlorite-illite	250-280
896-3066	Actinolite-epidote-wollastonite	>280

4.4 Stratigraphic and alteration mineralogical correlation of Wells OW-39A, OW-37A and OW-35A

4.4.1 Stratigraphic correlation

A geological cross-section extending from the southwest at Well OW-39A, through Well OW-37A and to Well OW-35 in the northwest (Figure 7) is shown in Figure 8. The lithology of the three wells shows the same type of rocks as those observed in other Olkaria wells (Musonye, 2012; Mwangi, 2012; Ronoh, 2012; Njathi, 2012). The top formation is composed of pyroclastic rock, which is very thin in Well OW-39A but thicker in Wells OW-37A and OW-35, indicating there could have been a flow forming thicker layers in the low lying areas of Wells OW-37A and OW-35. These pyroclasts overlie rhyolitic lavas in all the wells with subsequent layers of tuff, trachyte and basalt. Tuffs are common rocks in the three wells above 800 m, intercalating with basalt, rhyolite and trachyte; this could indicate that this area experienced phreatic episodes of eruptions in the past. Basalt occurs in the three wells with a thickness less than 50 m. Trachytes dominate the bottom depths in all the wells below 900, 750 and 700 m in Wells OW-39A, OW-37A and OW-35, respectively, intercalating with tuffs, rhyolite, basalts and minor intrusions. This could indicate the onset of the Plateau trachytes in these wells. The intrusions are only encountered in Wells OW-39A and OW-35. Basaltic and granitic intrusions occur only in Well OW-39A, whereas rhyolitic and syenitic intrusions occur in both wells (OW-39A and OW-35). There are no intrusions encountered in Well OW-37A. The occurrence of the intrusions in specific wells may imply that these intrusions are dykes. As has been discussed by earlier researchers on the subsurface geology of Olkaria (Browne, 1984; Leach and Muchemi, 1987; Muchemi, 1992; Omenda, 1998), a basaltic lava flow coincides with the cap rock of the reservoir and has been used as a marker horizon, as it is widespread. The basaltic lava was encountered at 808 m in Well OW-39A, 640 m in Well OW-37A;

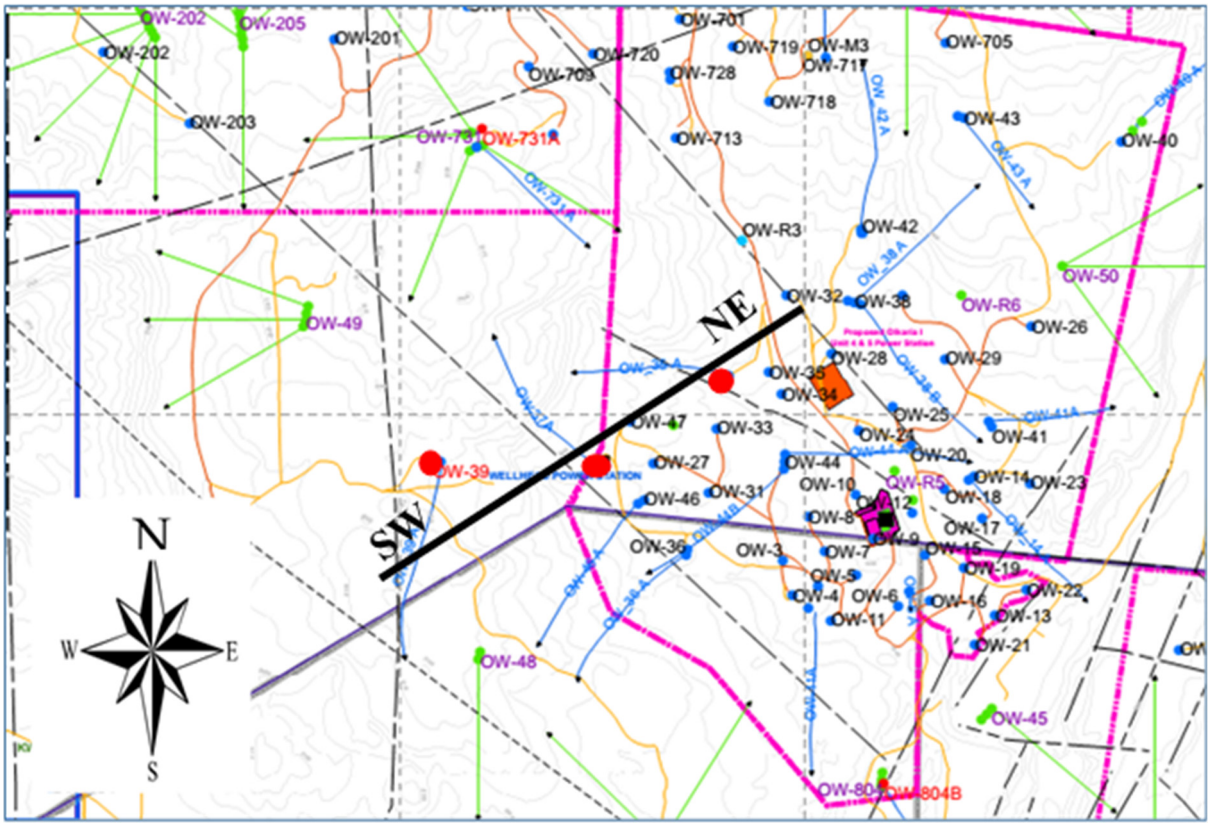

FIGURE 7: Cross cutting of correlation direction between
Wells OW-39A, OW-37A and OW-35A

OW-35 shows slightly variable depths of occurrence which may imply minor faulting. This, therefore, reveals the possible existence of a fault between Wells OW-39A and OW-37A, with the down throw towards Well OW-39A. The other fault could exist between Wells OW-37A and OW-35, with the down throw towards Well OW-35 (Figure 8).

4.4.2 Alteration mineral correlation

Isograds give a general picture of the temperature distribution in a geothermal system as they delineate the first appearance of an index mineral. The first appearance of index minerals was plotted (Figure 9) in all three wells and five distinct alteration zones were identified in all three. The top zone (unaltered zone) is quite thin in all the wells. The zeolite-smectite-illite zone appears at 2004 m a.s.l. in Well OW-39A, 1919 m a.s.l. in Well OW-37A and 1768 m a.s.l, in Well OW-35. This zone is thicker in Wells OW-39A and OW-37A and thinner in Well OW-35. The chlorite-illite zone appears at 1560 m a.s.l. in Well OW-39A, 1388 m a.s.l. in Well OW-37A and 1768 m a.s.l. in Well OW-35. This zone is thicker in Wells OW-37A and OW-35 but thinner in Well OW-39A. The first appearance of chlorite at these depths indicates alteration temperature of e 230°C. The first appearance of epidote is in basaltic lava at 1390 m a.s.l. in Well OW-39A, in a trachytic lava at 845 m a.s.l. in Well OW-37A and in tuff at 1288 m a.s.l. in Well OW-35, indicating that the alteration temperatures at these depths in the wells is 250°C. This temperature (250°C) is shallower in Wells OW-39A and OW-35 while deeper in Well OW-37A. The epidote zone is thinner in Well OW-39A and thicker in Well OW-35. Actinolite first appears in Well OW-39A at 1242 m a.s.l. Well OW-37A at 467 m a.s.l. and in Well OW-35 at 342 m a.s.l. The plots indicate that this zone is shallowest in Well OW-39A, indicating hotter shallow depth of alteration temperatures above 280°C. The correlation indicates elevation of the hydrothermal alteration in the area around Well OW-39A, implying the proximity of an upflow zone. Formation and alteration temperatures are within a similar range in Wells OW-37A and OW-35 but, in Well OW-39A, the formation and alteration temperatures are the reverse of each other, that is, the alteration temperature

indicates the proximity of upflow while the current formation temperature indicates marked cooling of the same structure. This might indicate a flow reversal of a specific permeability structure from a geothermal outflow to an inflow of cooler fluid into the geothermal system.

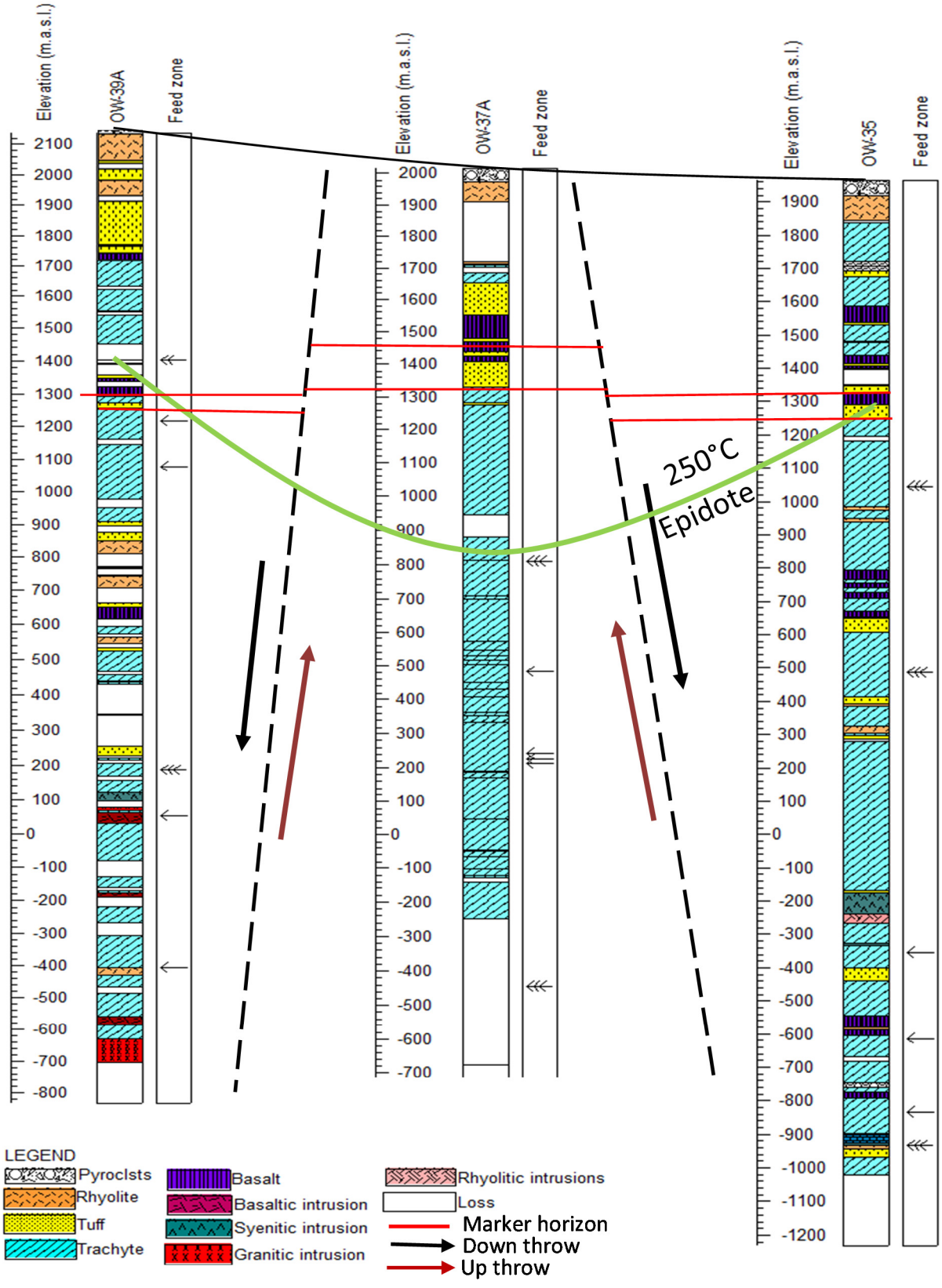

FIGURE 8: Stratigraphic correlation between Wells OW-39A, OW-37A and OW-35

4.5 Mineralogical evolution

The paragenetic sequences in hydrothermal systems are identified from cross-cutting veins and amygdale infilling sequences (Lagat, 2004). Paragenesis is the successive order in which minerals in a rock or a vein have crystallized. This successive sequence of mineral deposition is influenced by variations in pressure, temperature and the chemical composition of hydrothermal fluids that result in the precipitation of different hydrothermal alteration minerals at different times as conditions change in a geothermal reservoir. Therefore, compiling a paragenetic sequence with depth in a geothermal system assists in deciphering the detailed geologic geothermal history of the system. The mineral deposition sequence in vesicles and veins in Well OW-39A indicates a systematic increase in alteration temperatures, revealed by the deposition of low temperature minerals first, followed by high temperature ones. It was also observed that sequences at shallow depths consisted of low temperature minerals while high temperature mineral sequences were found at deeper levels. Table 3 shows the depositional sequences of hydrothermal alteration minerals in cuttings from Well OW-39A.

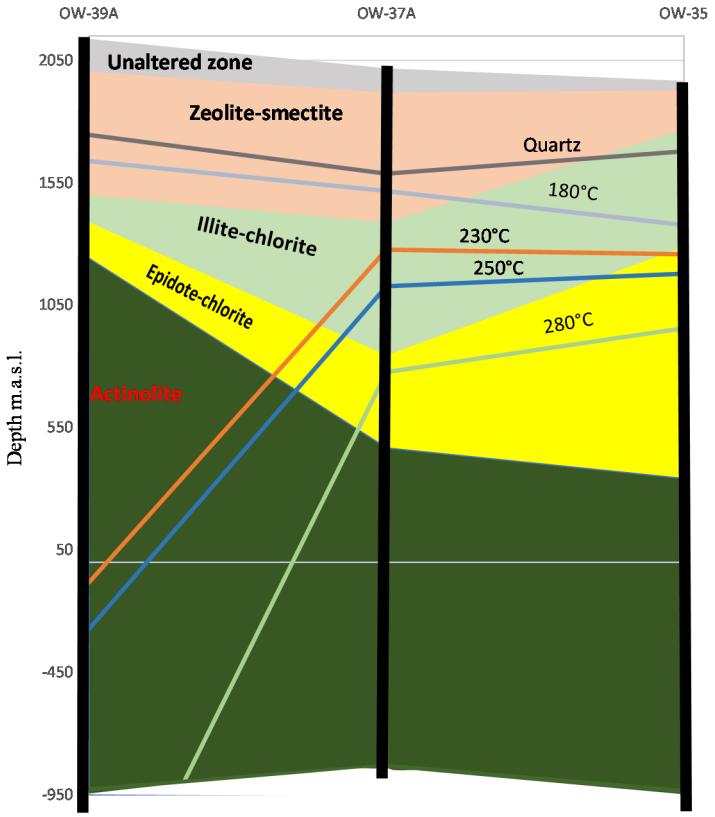

FIGURE 9: Alteration mineral correlation between Wells OW-39A, OW-37A and OW-35

4.6 Fluid inclusion geothermometry

Fluid inclusion analyses in Well OW-39A were done in quartz crystals. Fluid inclusion homogenization temperatures give the entrapment temperature of a fluid in a mineral (Roedder, 1984). This temperature, combined with other geochemical techniques, constrains potential sources and migration pathways and assists in deciphering the thermal history of a geothermal system. The homogenization temperatures (T_h) of the inclusions were measured in quartz crystals picked from 810 m depth and the results are presented in Figure 10. The T_h values ranged from 210-285°C in the quartz, apparently from two populations. The lower T_h value range is 210-215°C while the higher one ranges from 280-285°C. The lower range T_h values appear to be formed in healed fractures in the crystal and may have formed at a later stage than the higher ones which appeared more primary in nature. The high values may, therefore, be from an earlier phase, thus indicating that cooling had taken place in the geothermal system at this location.

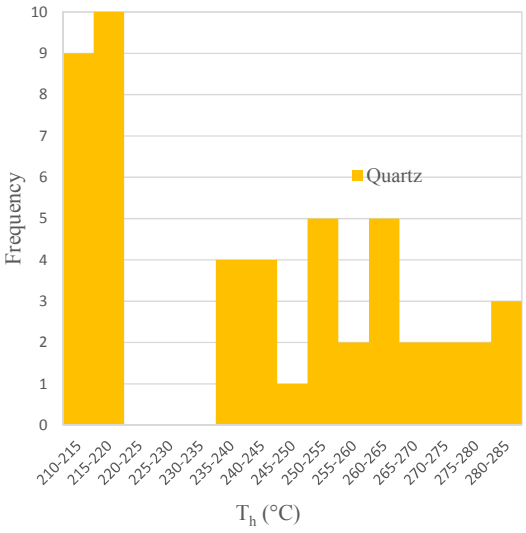

FIGURE 10: Histogram showing temperature and distribution of fluid inclusion

TABLE 3: Depositional sequences of hydrothermal alteration minerals in Well OW-39A

Depth (m)	Older ⟶ younger Sequence	Type
250	Zeolite » illite	Vein
402	Fluorite » illite	Vein
404	Zeolite » calcite » quartz » pyrite	Vesicle
438	Chalcedony » quartz » illite » platy »calcite	Vesicle
442	Zeolite » chalcedony » zeolite » quartz	Vein
448	Zeolite » calcite » clays	Vein
450	Pyrite » calcite	Vesicle
452	Chalcedony » zeolite	Vesicle
814	Quartz » chlorite » calcite	Vein
860	Chlorite » calcite	Vein
890	Chlorite » quartz» epidote	Vein
958	Quartz » chlorite	Vein
970	Quartz » chlorite	Vesicle
1114	Quartz » chlorite	Vein
1702	Quartz » epidote	Vein
2030	Quartz » chlorite » epidote	Vein
2240	Epidote » quartz	Vesicle
2288	Quartz » epidote	Vesicle
2602	Epidote » actinolite	Vesicle
2678	Epidote » actinolite	Vesicle
2698	Epidote » wollastonite	Vesicle

4.7 Comparison of measured, hydrothermal and fluid inclusion temperatures for Well OW-39A

Comparison of fluid inclusion, formation and alteration temperatures of Well OW-39A was done by plotting the formation temperature, mineral alteration temperatures and fluid inclusion data as shown in Figure 11. Comparisons between formation and alteration temperatures in a well are an important tool in determining the present geothermal condition of the well; they can indicate whether the well is cooling down, heating up or in equilibrium. In this well, alteration temperatures at 270, 392, 580, 748 and 896 m are 130, 180, 230, 250 and 280°C, respectively. The formation temperatures at 270, 392, 580, 748 and 896 m are 100, 150, 195, 205 and 210°C, respectively. The alteration temperatures at 270, 392, 580, 748 and 896 m are 30, 30, 45, 60 and 70°C, respectively, higher than the formation temperature, indicating the well is cooling. This difference increases with depth.

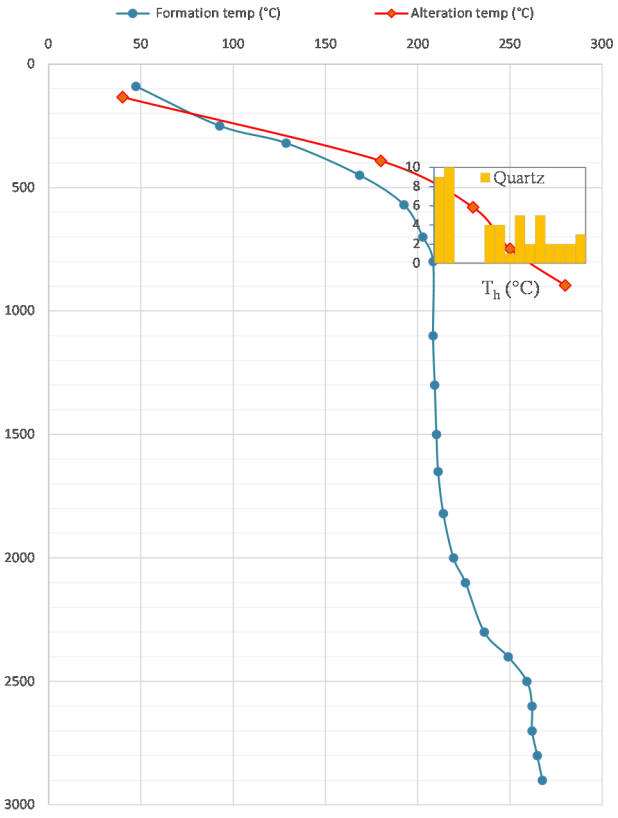

FIGURE 11: Comparison between fluid, fluid inclusion, alteration and formation temperatures of Well OW-39A

The homogenization temperature (T_h) values at 812 m in the well ranged from 210-285°C in the

quartz, as discussed above. The formation temperature at this depth is 208°C. The lowest T_h value range is 210-215°C while the highest is 280-285°C. These measurements indicate the inclusions (with lower T_h range 210-215°C) are near equilibrium with the current formation temperatures, whereas the high temperature range inclusions are far above the formation temperature. The formation temperature at 812 m is 208°C, indicating that the lower T_h range is in equilibrium with the current formation temperature, whereas the highest T_h range is far above the formation temperature. The two sets of T_h temperatures reveals two geothermal histories of the well; at one time elevated temperature existed, succeeded by cooling. In this discussion, we assume that the measured temperature conforms to the formation temperature.

4.8 Aquifers and permeable zones

The main sources of permeability in the Greater Olkaria volcanic complex are lithological contacts, intrusive boundaries and major faults and fractures (Lagat, 2004; Gylfadóttir et al., 2011). Permeability and feed zones in Well OW-39A (Table 4) were identified and interpreted by monitoring the loss of circulation fluid during drilling, hydrothermal alteration mineralogy patterns, changes in circulating fluid temperature and temperature recovery tests (Figure 12). The temperature logs and alteration intensity reveal that the well is highly permeable above 2250 m. The feed zones in this well were identified in the production zone and are classified as major, minor, and intermediate. Four minor aquifers occurring at 950, 1500, 1800, 2250 and 2750 m are marked by high intensity of alteration fracturing and loss of returns. Two intermediate aquifers occur at 750 and 1100 m. At 750 m, there is a marked loss of circulation and high intensity of alteration while at 1100 m, there is high alteration intensity, veining and fracturing. The major aquifer at 2100 m is marked by lithological contact between intrusions, loss of circulation and fracturing.

TABLE 4: Interpreted permeable zones / aquifers based on geological observations

Depth (m)	Evidence geological observation
696	Loss of circulation
748	Loss of circulation with high intensity of rock alteration calcite and pyrite deposition, fracturing of trachyte lava
950	Alteration intensity and highly fractured rock, veining and oxidation
1008	Loss of circulation
1100	High intensity of alteration, increase in oxidation and fracturing
1500	Loss of circulation
1550	Primary porosity, and high intensity of alteration
1602	Loss of circulation
1800	Loss of circulation, fracturing
2100	Lithological contact between syenite and trachyte, intrusion, veining and fracturing alteration
2250	Lithological contact between basaltic intrusion and trachyte, veining, fracturing and increased amount of calcite
2750	Lithological contact between rhyolite and trachyte

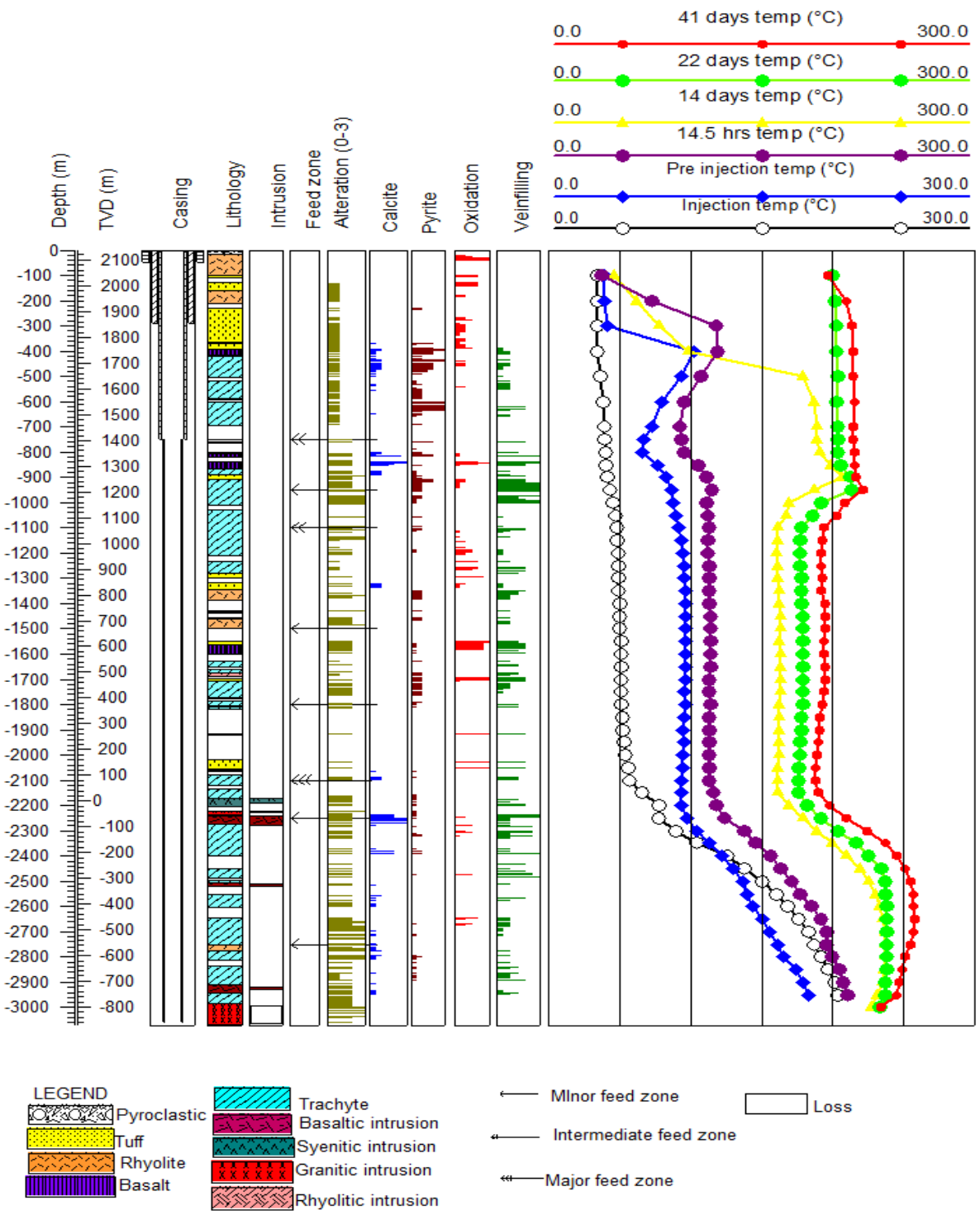

FIGURE 12: Feed zones in Well OW-39A in relation to the geological evidence and the recovery and circulation fluid temperature measurements

5. DISCUSSION AND INTERPRETATION

The lithology of Well OW-39A was interpreted by analysis of the drill cuttings from the well, using binocular and petrographic microscopes. From these analyses, five main rock types, namely pyroclastics, tuffs, rhyolites, basalts and trachytes, were encountered in the well. Pyroclastic rocks form the uppermost 14 m; the underlying rhyolites extend to 98 m and correspond to the Olkaria comendites. Rhyolitic tuffs and basalts dominate the upper 400 m of the stratigraphic column of the well, representing the Upper Olkaria volcanics, while Plateau trachytes dominate at depth and form the main reservoir formation. Hence, the stratigraphy of Well OW-39A relates well with the general stratigraphic column of the Greater Olkaria volcanic complex (Shackleton, 1986; Ogoso-Odongo, 1986; Omenda, 2000).

Stratigraphic correlation between Wells OW-39A, OW-37A and OW-35 show that the pyroclastic deposit forms a very thin layer in Well OW-39A, but is thicker (44-48 m) and of almost equal thickness in Wells OW-37A and OW-35, implying the pyroclastic deposit could have been a flow deposit formed by erosion of a higher elevated area (Well OW-39A) resulting in thicker layers in the low lying areas (Wells OW-37A and OW-35). Rhyolites appear near the surface in all three wells, underlying the pyroclasts and extending to 98 m in Well OW-39A, 304 m in Well OW-37A and 122 m depth in Well OW-35. These are the comenditic lavas and their occurrence conforms to the Olkaria stratigraphic column. Tuff is a common rock in the three wells above 800 m. It first occurs below the rhyolites in Well OW-39A and below the trachytes in both Well OW-37A and Well OW-35, intercalating with basalt, rhyolite and trachyte; this could indicate that this area experienced phreatic eruptions in the past. Basalt occurs in the three wells with a thickness of less than 50 m. The uppermost occurrence was first noted at 392 m in Well OW-39A, 468 m in Well OW-37A and 380 m in Well OW-35. This basalt layer can be used as a marker horizon when carrying out analyses of drill cuttings to infer buried faults in this area. However, the depth of the basalt also often corresponds to the cap rock of the geothermal reservoir. Below the Olkaria basalts, trachyte is the dominant rock in the wells. At greater depth, it was observed to be the dominant rock below 900, 750 and 700 m in Wells OW-39A, OW-37A and OW-35, respectively, intercalating with minor thin layers of tuff, basalt and rhyolite along with minor intrusives, although intercalations of tuffs, basalts, rhyolites and intrusives were absent in Well OW-37A. This also relates to the Plateau trachytes which were noted to occur in the Olkaria geothermal complex at a depth between 1000 and 2600 m. Intrusives were only encountered in Wells OW-39A and OW-35 at depth. Apart from the granitic intrusion encountered at the bottom of Well OW-39A, the other intrusives ranged from 8 to 30 m in apparent thickness. Basaltic and granitic intrusions occur only in Well OW-39A, whereas rhyolitic and syenitic intrusions occur in both wells (OW-39A and OW35). There was no intrusion encountered in Well OW-37A. The occurrence of the intrusions in specific wells could probably imply that some of these intrusions are dykes. The occurrence of fresh rhyolitic dykes implies a young age, possibly related to the Ololbutot eruptive fissure. The presence of a thick granitic intrusion (~80 m) at depth could signify a more substantial intrusion and serve as a local heat source at depth, as was postulated by Gylfadóttir et al. (2011) when interpreting possible heat sources (below Olkaria hill, Gorge farm volcanic centre and domes), based on the seismic attenuation data of the Olkaria geothermal system.

Taking into consideration the topographic correction between the wells, true vertical depth with reference to the elevation of each well was used. Stratigraphic correlation of the basalt layers between the three wells indicates the possible existence of normal faults between Wells OW-39A/OW-37A and OW-37A/OW35, with downthrows towards Wells OW-39A and OW-35, respectively. Also the appearance of dominant trachyte below 900, 750 and 700 m in Wells OW-39A, OW-37A and OW 35, respectively, correlates well with the probable existence of normal faults, as shown in Figure 8, and hence conforms to observations made by Lagat (2004).

Permeability in Well OW-39A is very high, characterised by high fracturing, veining, the intensity of alteration, and circulation losses. The presence of calcite and the abundance of pyrite in this well indicate high past or present permeability. The well also shows high oxidation, indicating there were

channels/fractures of oxygen rich fluid flow in the rocks. Aquifer information is determined through the analysis of temperature logs run during and after completion of the well. Circulation losses/gains and alteration data play important roles in positioning aquifers. The aquifers in Well OW-39A were determined from temperature logs and are mainly associated with a high intensity of alteration, lithological boundaries, fractures and highly fractured rocks. Two intermediate aquifers occur at 750 and 1100 m. At 750 m, the aquifer is marked by a loss of circulation and high intensity of alteration, while at 1100 m (in trachyte), the aquifer is defined by high alteration intensity, veining and fracturing. From the interpretation of the temperature profile, this aquifer (1100 m) could be a channel of cold fluids into the well. A major aquifer at 2100 m is associated with an intrusion of syenitic composition, but fracturing was observed at the intrusion contact. In Well OW-37A, major aquifers were noted in trachyte at 1250 m, marked by circulation losses, fracturing and high intensity of alteration and at 2600 m, by loss of circulation. In Well OW-35, three major aquifers were identified. At 980 and 1480 m, the aquifers were marked by high intensity of alteration, an abundance of pyrite, oxidation and veining, while at 2900 m the aquifer was marked by fracturing, intrusives, veining and lithological contact between rhyolite and syenitic intrusions.

Hydrothermal alteration minerals were observed in the veins, vugs and vesicles and as a replacement of primary minerals. Their distribution in active geothermal fields depends on the ability of fluid to approach equilibrium in host rocks at any scale during the hydrothermal processes. In this well (OW-39A), the appearance of smectite (134, 384 m) and kaolinite (572 m) indicate temperatures of less than 200°C, whereas kaolinite indicates the presence of acidic fluids. Illite and chlorite are the dominant clay minerals in this well, appearing down to the well bottom.

The study of the hydrothermal distribution pattern shows five distinct alteration zones with the first appearance of the index minerals coinciding with the upper boundary of each zone. These are: the unaltered zone (0-134 m) that has no alteration related to geothermal activity, suggesting temperatures of <40°C. The second zone (zeolite-smectite zone) that extends from 134 to 578 m is the lowest grade mineral alteration zone, indicating alteration temperatures of <200°C. It is characterised by high oxidation and abundant zeolites. The third zone (chlorite-illite zone), which is marked by the first appearance of chlorite, occurs between 578 and 748 m. The zone is fractured as evidenced in the veining and is characterised by an abundance of pyrite and calcite, suggesting the zone is highly permeable. Epidote-chlorite-illite is the fourth zone, extending from 748 to 896 m. The top depth is marked by the first appearance of epidote and is characterised by high oxidation, veining, high intensity of alteration, and an abundance of pyrite and calcite, indicating that the zone is also highly permeable. The appearance of epidote in this zone indicates that the alteration temperature at 748 m and below could be above 250°C. Other minerals present in this zone include albite, prehnite, sphene, quartz, chlorite, illite, fluorite, pyrite, calcite and oxides. The fifth zone extends from 896 m to the bottom of the well. It is marked by the first appearance of actinolite at 896 m, indicating temperatures above 280°C below this depth. It is characterised by the mineral assemblage of actinolite, wollastonite, epidote and prehnite. Other minerals in this zone include pyrite, calcite, fluorite, chlorite, illite, and oxides. The absence of actinolite for a long interval between 1488 and 2210 m in the well could indicate the absence of favourable conditions, such as high temperature, for the formation of actinolite.

Successive sequences of mineral deposition in vesicles and veins is influenced by variations in pressure, temperature and the chemical composition of hydrothermal fluids that result in the precipitation of different hydrothermal alteration minerals at different times (Reyes, 2000). In Well OW-39A, it was observed that sequences at shallow depths consisted of low temperature minerals while a high temperature mineral sequence was found at depths below 890 m. The mineral deposition sequence in the veins and vesicles showed systematic gradation from low to high temperature minerals throughout the well, implying that the low temperature minerals were older as they were deposited first and the subsequent high temperature minerals were younger. This reveals that during the deposition of these minerals, the geothermal system around the well was heating up.

The homogenization temperature (T_h) values, analysed from fluid inclusions in a quartz vein from 812 m in Well OW-39A, ranged from 210 to 285°C, but formed two populations; the lower T_h value range is 210-220°C, while the higher one is 235-285°C. For comparison, the measured (formation) temperature at this depth is 208°C. Inclusions in the healed fractures had a T_h range of 210-220°C, representing current conditions, while the primary inclusions had a T_h range of 235-285°C. These measurements indicate that the inclusions with lower T_h range (210-220°C) are near equilibrium with the current formation temperatures, whereas the high-temperature range (235-285°C) inclusions are far above the formation temperature, but in equilibrium with the alteration temperature. The wide range in T_h temperature reveals two geothermal phases in the proximity of the well, meaning the temperature was higher than 280°C at one point in time, but has since cooled to ~210°C. Alteration temperature is far above the formation temperature below 392 m (Figure 10) indicating the reservoir is cooling below this depth.

The alteration mineral correlation between Wells OW-39A, OW-37A and OW-35 (Figure 9) indicates that the chlorite-illite zone is thinner in Well OW-39A while it is thicker in Wells OW-37A and OW-35, implying a higher temperature gradient with depth in Well OW-39A. Epidote occurs at a shallower depth in Wells OW-39A (1390 m a.s.l.) and OW-35 (1288 m a.s.l.), but deeper in Well OW-37A (845 m a.s.l.). This zone is thicker in Well OW-35 than in the other two wells. Actinolite appears at the shallowest depth in Well OW-39A and deeper in Well OW-35A, hence the actinolite zone is thicker in Well OW-39A. The plots indicate that this shallow zone in Well OW-39A indicates higher alteration temperatures at shallow depth, possibly caused by an upflow zone and higher permeability around Well OW-39A. Formation and alteration temperatures are within the same range, i.e. almost at equilibrium in Wells OW-37A and OW-35 but, in Well OW-39A, formation and alteration temperature are reversed. That is, the alteration temperature indicates a previous upflow zone in the vicinity around this well, while the current formation temperature indicates a reversal in temperature, probably due to cold water inflow and mixing.

Well OW-39A was drilled directionally to the south, adjacent to the Ololbutot fault which is a N-S trending eruptive fissure which erupted approximately 180±50 yrs. (Clarke et al., 1990). Gylfadóttir et al. (2011) noted that this fault appears to represent a long term groundwater flow structure breaking through the hydrological barrier that the Olkaria region forms, south of Lake Naivasha. Permeability connected to the groundwater systems can also shape the alignment of the thermal reservoir, as is postulated as being the cause of the separation between Olkaria West and East (Ololbutot fissure). Observations made from oxidation trends, veining and temperature logs in Well OW-39A indicate that the well is highly fractured and that these fractures act as groundwater flow channels in the rock formations. Also, the reversal in alteration (through fluid inclusion analysis) and formation temperatures (Figure 12) observed in the well indicates that the fluid flow in the area around the well has been reversed using the same geothermal structure, implying an old hot geothermal structure reversed to a "cold geothermal barrier" which has resulted in cooling of Well OW-39A. Observations made from hydrothermal alteration mineralogy and a mineral deposition sequence do not show a temperature reversal, hence, signs of cooling are not evident. This could probably imply that the cooling of the area around the well is a recent event.

6. CONCLUSIONS

- The lithology of Well OW-39A is composed of pyroclastics, tuffs, rhyolites, basalts, trachytes and minor basaltic, rhyolitic, syenitic and granitic intrusions. The rock types conform to the general geology of Olkaria.
- The thick (~80 m apparent thickness) granitic intrusion could originate from a deeper granitic body which may be a heat source.
- Stratigraphic correlation of Wells OW-39A, OW-37A and OW-35 indicates the possible existence of a normal fault between Wells OW-39A and OW-37A, and Wells OW-37A and OW-35.

- Hydrothermal alteration mineral assemblages and their distribution in the well are mainly controlled by temperature, rock type, fluid composition and permeability. Low temperature minerals were found in the upper part while high temperature minerals reside in the deeper part.
- Mineral depositional sequences in vesicles and veins in the well show systematic gradation of hydrothermal alteration minerals, ranging from low temperature to high temperature, indicating a history of heating in the reservoir.
- Five alteration zones were identified, based on hydrothermal mineral assemblages. These include: an unaltered zone (0-134 m); a zeolite-smectite-illite zone (134-578 m); a chlorite-illite zone (578-748 m); an epidote-chlorite zone (748-896 m); and an actinolite-epidote-wollastonite zone (896-3066 m).
- Temperature profile monitoring and geological evidence indicate Well OW-39A is highly permeable above 2250 m.
- Aquifers in this well show a close association with circulation losses, fractured formations, and lithological contacts between the formation and intrusions at depth. High past and present permeability in this well is indicated by the high abundance of pyrite and calcite, high alteration intensity, high oxidation, fracturing and the high occurrence of veins. High oxidation in this well may also indicate groundwater flow in the fractures in the area around the well.
- Comparison between fluid inclusion, alteration, and formation temperature indicate evidence of two geothermal phases in proximity to the well; the first phase of elevated temperatures is succeeded by a cooling phase. Hence, the well is cooling.
- Alteration zones in Well OW-39A show a marked elevation compared to neighbouring Wells OW-37A and OW-35, suggesting that the well is nearer to an upflow zone than the others. However, a comparison of the formation temperatures of the same wells show much lower temperatures in Well OW-39A, indicating that the upflow channel in proximity to the well may now be acting as an inflow of cooler fluids from outside of the geothermal system. An assumption was made that the measured temperature in the well is the same as the formation temperature.
- Observations made from hydrothermal alteration mineralogy and the mineral deposition sequence did not show a temperature reversal, hence, signs of cooling were not evident. This might imply that the cooling of the area around the well is a recent event, possibly younger than the Ololbutot eruptive fissure.

ACKNOWLEDGEMENTS

My first sincere gratitude is expressed to the United Nations University Geothermal Training Programme (UNU-GTP) and the Government of Iceland for granting me this opportunity to study and widen my understanding of geothermal energy. Special thanks go to the former director of the UNU-GTP, Dr. Ingvar B. Fridleifsson, Mr. Lúdvík S. Georgsson, director, Ms. Thórhildur Ísberg, Mr. Ingimar G. Haraldsson, Mr. Markús A. G. Wilde and Málfrídur Ómarsdóttir, for their coordinated assistance to smoothly see me through this course. I extend my gratefulness to my supervisors, Ms. Anette K. Mortensen, Dr. Björn S. Hardarson and Dr. Hjalti Franzson, for their tireless technical assistance, dedication and availability during the entire project time. Thanks go to Sigurdur Sveinn Jónsson for his assistance in interpretation of X-RD data and to all other ISOR staff.

I would also like to thank my employer, Kenya Electricity Generating Company (KenGen), for granting me the opportunity to attend this course. Special thanks go to my fellow borehole geologists, Tito, Loice and Claudia, for their immense support during the project. To the 2013 UNU fellows, thanks for creating a conducive environment that made me feel at home.

Special thanks go to parents, my husband, and my children for their endless love, moral support, encouragement and prayers during the six months period.

Finally, I wish to express my heartfelt gratitude to the almighty God for giving me strength and for how far he has brought me.

REFERENCES

Ambusso, W.J. and Ouma, P.A., 1991: Thermodynamic and permeability structure of Olkaria Northeast field: Olkaria fault. *Geothermal Resource Council, Trans., 15,* 237-242.

Baker, B.H., and Wohlenberg, J., 1971: Structural evolution of the Kenya Rift Valley. *Nature, 229*, 538-542.

Baker, B.H, Mohr, P.A, and Williams, L.A.J., 1972: Geology of the Eastern Rift System of Africa. *Geological Society of America, Special Paper 136,* 1-67.

Baker, B.H., Williams, L.A.J., Miller, J.A., and Fitch, F.J., 1971: Sequence and geochronology of the Kenya Rift volcanics. *Tectonophysics, 11*, 191-215.

Browne, P.R.L., 1978: Hydrothermal alteration in active geothermal fields. *Annual Review Earth & Planetary Sciences,* 6, 229-250.

Browne, P.R.L., 1984: Subsurface stratigraphy and hydrothermal alteration of the eastern section of the Olkaria geothermal field, Kenya. *Proceedings of the 6th New Zealand Geothermal workshop, Geothermal Institute, Auckland,* 33-41.

Browne, P.R.L., and Ellis, A.J., 1970: The Ohaki-Broadlands hydrothermal area, New Zealand: mineralogy and related geochemistry. *Am. J. Sci., 269*, 97-131.

Clarke, M.C.G., Woodhall, D.G., Allen, D., and Darling G., 1990: Geological, volcanological and hydrogeological controls on the occurrence of geothermal activity in the area surrounding Lake Naivasha, Kenya, with coloured 1:100 000 geological maps. Ministry of Energy, Nairobi, 138 pp.

Franzson, H., 1998: Reservoir geology of the Nesjavellir high-temperature field in SW-Iceland. *Proceedings of the 19th Annual PNOC-EDC Geothermal Conference, Manila,* 13-20.

Franzson, H., 2013: *Borehole geology*. UNU-GTP, Iceland, unpublished lecture notes.

Gylfadóttir, S.S., Halldórsdóttir, S., Arnaldsson, A., Ármannsson, H., Árnason, K., Axelsson, G., Einarsson, G.M., Franzson, H., Fridriksson, Th., Gudlaugsson, S.Th., Gudmundsson, G., Hersir, G.P., Mortensen, A.K. and Thordarson, S., 2011: *Revision of the conceptual model of the Greater Olkaria geothermal system-phase I.* Mannvit/ÍSOR/Vatnaskil/Verkís Consortium, report, Reykjavík, 100 pp.

Harvey, C.C., 1998: *The application of clay mineralogy to the exploration and development of hydrothermal resources*. Geothermal Institute, University of Auckland, NZ, unpublished lecture notes.

Haukwa, C.B., 1984: *Recent measurements within Olkaria East and West fields*. Kenya Power Co., internal report, 13 pp.

Kristmannsdóttir, H., 1979: Alteration of basaltic rocks by hydrothermal activity at 100-300°C. In: Mortland, M.M., and Farmer, V.C. (editors), *International Clay Conference 1978*. Elsevier Scientific Publishing Co., Amsterdam, 359-367.

Lagat, J.L., 1998: *Borehole geology of well OW-801, Olkaria South East Field*. KenGen, Kenya, internal report, 12 pp.

Lagat, J.L., 2004: *Geology, hydrothermal alteration and fluid inclusion studies of Olkaria domes geothermal field, Kenya.* University of Iceland, MSc thesis, UNU-GTP, Iceland, report 2, 71 pp.

Lagat, J., 2007: *Borehole geology of OW-904A*. KenGen, Kenya, internal report.

Leach, T.M., and Muchemi G.G., 1987: Geology and hydrothermal alteration of the North and West exploration wells in the Olkaria geothermal field, Kenya. *Proceedings of the 9th New Zealand Geothermal Workshop, Geothermal Institute, Auckland,* 187-192.

MacDonald, R., Black, H.E., Fitton, J.G., Marshall, A.S., Nejbert, K., Rodgers, N.W., and Tindle, A.G.,

2008: The roles of fractional crystallization, magma mixing, crystal mush remobilization and volatile melt interactions in the genesis of a young basalt-peralkaline rhyolite suite, the Greater Olkaria volcanic complex, Kenya Rift Valley. *J. Volcanology, 49-8*, 1515-1547.

MacDonald, R., Black, S., Fitton, J.G., Rogers, N.W., and Smith, M., 2001: Plume-lithospheric interactions in the generation of the basalts of the Kenya Rift, East Africa. J. *Petrology, 42*, 877-900.

MacDonald, R., Davies, G.R., Bliss, C.M., Leat, P.T., Bailey, D.K., and Smith, R.L., 1987: Geochemistry of high silica peralkaline rhyolites, Naivasha, Kenya rift valley. *J. Petrology, 28*, 979-1008.

Marshall, A.S.L., Macdonald, R., Rogers, N.W., Fitton. J.G., Tindle, A.G.N., Nejbert, K., and Khinton, R.W., 2009: Fractionation of peralkaline silicic magmas: The Greater Olkaria volcanic complex, Kenya Rift valley. *J. Petrol., 50,* 323-359.

Mathews, A., 1976: Magnetite formation by the reduction of hematite with iron under hydrothermal conditions. *American Mineralogist, 61,* 927-932.

Mosley, P.N., 1993: Geological evolution of the late Proterozoic "Mozambique belt" of Kenya. *Tectonophysics, 221*, 223-250.

Muchemi, G.G., 1992: *Geology of the Olkaria North East field KPC*. KenGen, Kenya, internal report.

Muchemi, G.G., 2000: *Conceptual model of Olkaria geothermal field. KenGen, Kenya.* KenGen, internal report.

Mungania, J., 1992: *Preliminary field report on geology of Olkaria volcanic complex with emphasis on Domes area field investigations*. Kenya Power Company, internal report.

Mungania, J., 1999: *Geological report of well OW-714.* Kenya Power Company, Kenya, internal report.

Musonye, X.S., 2012: Borehole geology and alteration mineralogy of well OW-914A, Domes area Olkaria geothermal field. Report no 23 in: *Geothermal training in Iceland*, 501-540.

Mwangi, D. W., 2012: Borehole geology and hydrothermal mineralization of well OW-916, Domes geothermal field. Report no 24 in: *Geothermal training in Iceland*, 541-571.

Mwania, M., Munyiri, S., and Okech, E., 2013: Borehole geology and hydrothermal mineralisation of well OW-35, Olkaria East geothermal field, Central Kenya Rift Valley. Report 1 in: *Geothermal training in Kenya*. UNU-GTP, Iceland, 1-56.

Naylor, W.I. 1972: *The geology of Eburru and Olkaria geothermal prospects*. UNDP project report, KPC, 58 pp.

Njathi, D.W., 2012: Borehole geology and hydrothermal mineralization of well OW-911A, Olkaria Domes geothermal field, Kenya. Report no 25 in: *Geothermal training in Iceland*. UNU-GTP, Iceland, 573-600.

Ogoso-Odongo, M.E., 1986: Geology of Olkaria geothermal field. *Geothermics, 15,* 741-748.

Omenda, P. A., 1990: *Geological report for Olkaria well OW-305*. KPC internal report.

Omenda, P.A., 1994: The geological structure of the Olkaria west geothermal field, Kenya. *Proceedings of the 19th Stanford Geothermal Reservoir Engineering Workshop, Stanford, Ca*, 125-130.

Omenda, P.A., 1998: The geology and structural controls of the Olkaria geothermal system, Kenya. *Geothermics, 27-1,* 55-74.

Omenda, P.A., 2000: Anatectic origin for comendite in Olkaria geothermal field, Kenya Rift; Geochemical evidence for syenitic protholith. *African J. Science and Technology. Science and Engineering Series, 1*, 39-47.

Omenda, P.A., 2007: The geothermal activity of the East African rift. *Presented at Short Course II on Surface Exploration for Geothermal Resources, organised by UNU-GTP and KenGen, at Lake Naivasha, Kenya,* 12 pp.

Onacha, S.A., 1993: *Resistivity studies of the Olkaria-Domes geothermal project*. Kenya Power Company, internal report.

Otieno, V., and Kubai, R., 2013: Borehole geology and hydrothermal mineralisation of well OW-37A, Olkaria East geothermal field. Report 2 in: *Geothermal training in Kenya*. UNU-GTP, Iceland, 57-105.

Pendon, R.R., 2006: *Borehole geology and hydrothermal mineralisation of well HE-22, Ölkelduháls field, Hengill area, SW-Iceland*. Report 17 in: *Geothermal training in Iceland 2006*. UNU-GTP,Iceland, 357-390.

Reyes, A.G., 2000: *Petrology and mineral alteration in hydrothermal systems. From diagenesis to volcanic catastrophes.* UNU-GTP, Iceland, report 18-1998, 77 pp.

Roedder, E., 1984: *Fluid inclusions*. Mineral. Soc. Am., Rev. Mineral., 12, Washington, DC, 644 pp.

Ronoh, I.J., 2012: Borehole geology and hydrothermal alteration of well OW-912B, Olkaria Geothermal field, Central Kenya Rift Valley. Report no 25 in: *Geothermal training in Iceland*, 695-732.

Ryder, A.J.D., 1986: *Geological report of well OW-701 Olkaria geothermal field, Kenya.* KenyaPower Company report, prepared by GENZL.

Saemundsson, K., and Gunnlaugsson, E., 2002: *Icelandic rocks and minerals*. Edda and Media Publishing, Reykjavík, Iceland, 233 pp.

Shackleton, R.M., 1986: Precambrian collision tectonics in Africa. In: Coward, M.P., and Ries, A.C., *Collision Tectonics, Geological Society Special Publication*, 19, 329-249.

Simiyu, S.M., 1996: *Integrated geophysical study of the southern Kenya rift*. University of Texas, El Paso, PhD thesis.

Simiyu, S.M., and Keller, G.R., 1997: Integrated geophysical analysis of the East African Plateau from gravity anomalies and recent seismic studies. *Tectonophysics, 278,* 291-314.

Simiyu, S.M., Oduong, E.O., and Mboya, T.K., 1998: *Shear wave attenuation beneath the Olkaria volcanic field.* KenGen, Kenya, internal report, 29 pp.

Simmons, S F., and Christenson, B.W., 1994: Origins of calcite in boiling geothermal system. *American Journal of Science, 294* 361-400.

Smith, M., 1994: Stratigraphic and structural constraints on mechanisms of active rifting in the Gregory Rift, Kenya.*Tectonophysics, 236*, 3–22.

Smith, M., and Mosley, P., 1993: Crustal heterogeneity and basement influence on the development of the Kenya rift, East Africa. *Tectonics, 12*, 591-606.

Thiessen, R., Burke, K. and Kidd, W.S.F., 1979: African hotspots and their relation to the underlying mantle. *Geology*, *7*, 263-266.

Thompson, A.O., and Dodson, R.G., 1963: *Geology of the Naivasha area*. Geological Survey of Kenya, Kenya, report 55.

Wheeler, W.H., and Karson, J.A., 1994: Extension and subsidence adjacent to a ‘‘weak’’ continental transform: an example of the Rukwa Rift, East Africa. *Geology, 22,* 625-628.

Virkir Consulting Group, 1980: *Geothermal development at Olkaria*. Report prepared for Kenya Power Company.

APPENDIX I: XRD analysis from Well OW-39A

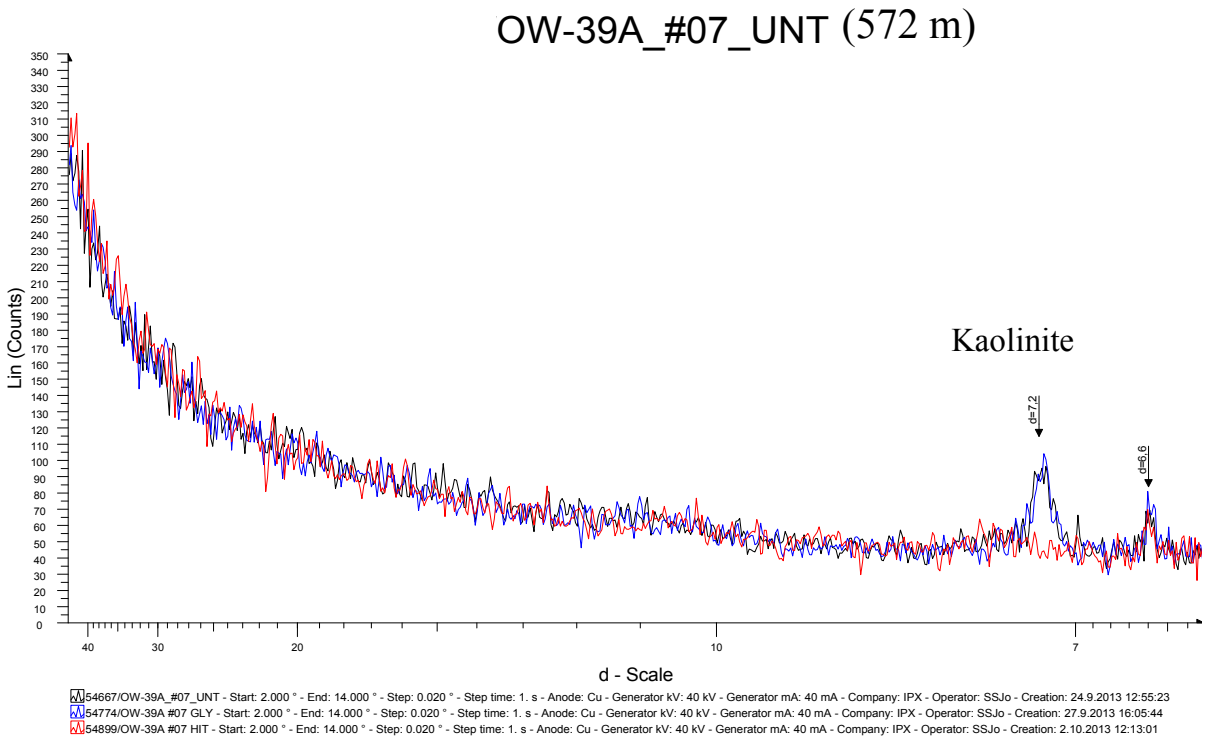

FIGURE 1: XRD analysis showing kaolinite peak

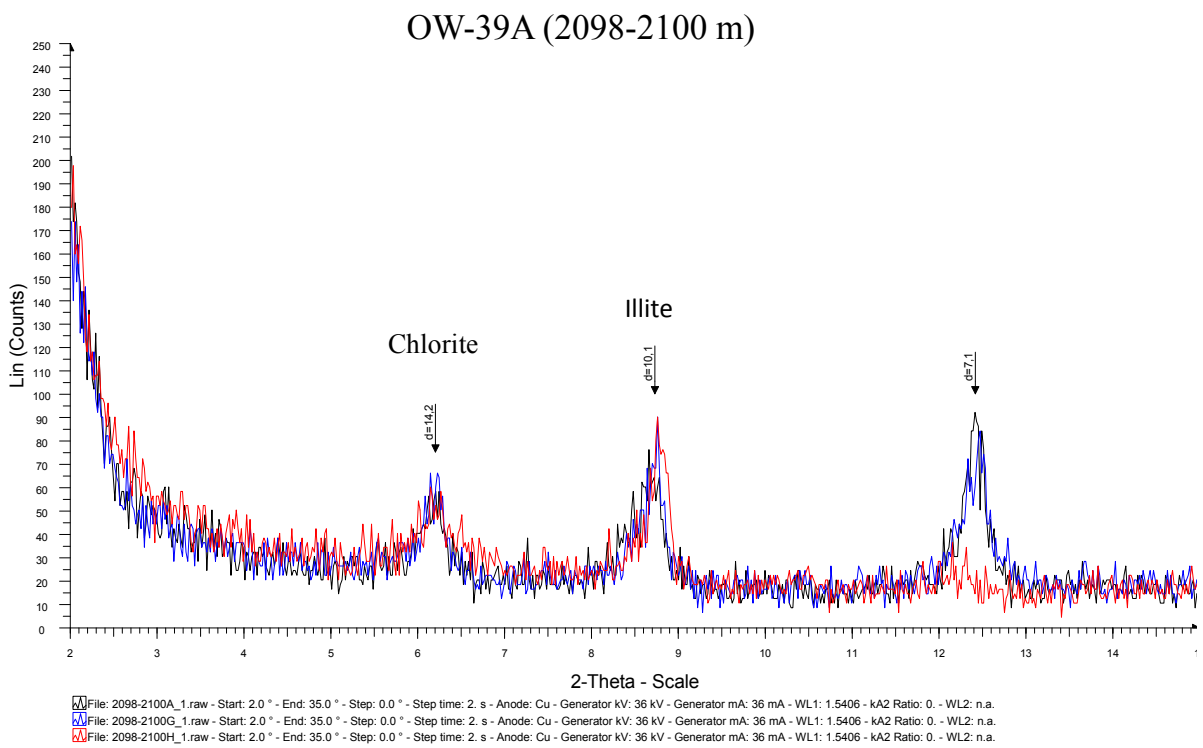

FIGURE 2: XRD analysis showing chlorite and illite peaks